Science of the Total Environment 780 (2021) 146581

Contents lists available at ScienceDirect

Science of the Total Environment

journal homepage: www.elsevier.com/locate/scitotenv

Nitrogen isotopes in the soil-to-tree continuum — Tree rings express the soil biogeochemistry of boreal forests exposed to moderate airborne emissions

Martine M. Savard [a,*], Christine Martineau [b], Jérôme Laganière [b], Christian Bégin [a], Joëlle Marion [a], Anna Smirnoff [a], Franck Stefani [c], Jade Bergeron [a], Karelle Rheault [b], David Paré [b], Armand Séguin [b]

[a] Geological Survey of Canada, Natural Resources Canada, 490 rue de la Couronne, Québec, QC G1K 9A9, Canada
[b] Canadian Forest Service, Laurentian Forestry Centre, 1055 rue du P.E.P.S., Stn. Sainte-Foy, P.O. Box 10380, Québec, QC G1V 4C7, Canada
[c] Agriculture and Agri-Food Canada, 960 Avenue Carling, Ottawa, ON K1A 0C6, Canada

HIGHLIGHTS

- Studied forests exposed to different rates and $\delta^{15}N$ values of airborne N inputs
- $\delta^{15}N$ values studied in the soil-to-tree N continuum
- Air $\delta^{15}N$ values not transferred to trees as no direct change to used up soil N
- Airborne N possibly influences soil N transformation and microbial communities.
- Tree-ring $\delta^{15}N$ values reflect soil pH and possibly levels of anthropogenic N inputs.

GRAPHICAL ABSTRACT

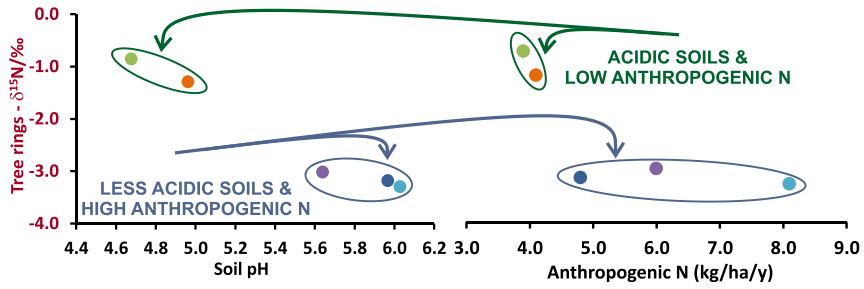

ARTICLE INFO

Article history:
Received 11 January 2021
Received in revised form 15 March 2021
Accepted 15 March 2021
Available online 20 March 2021

Editor: Elena Paoletti

Keywords:
Reactive N
pH
Ectomycorrhizal fungi
Soil microbiome
N transformation
Airborne pollutants

ABSTRACT

Anthropogenic N emissions represent a potential threat for forest ecosystems, and environmental indicators that provide insight into the changing forest N cycle are needed. Tree ring N isotopic ratios ($\delta^{15}N$) appear as a contentious choice for this role as the exact mechanisms behind tree-ring $\delta^{15}N$ changes seldom benefit from a scrutiny of the soil-to-tree N continuum. This study integrates the results from the analysis of soil chemistry, soil microbiome genomics, and $\delta^{15}N$ values of soil N compounds, roots, ectomycorrhizal (EcM) fungi and recent tree rings of thirteen white spruce trees sampled in five stands, from two regions exposed to moderate anthropogenic N emissions (3.9 to 8.1 kg/ha/y) with distinctive $\delta^{15}N$ signals.

Our results reveal that airborne anthropogenic N with distinct $\delta^{15}N$ signals may directly modify the NO_3^- $\delta^{15}N$ values in surface soils, but not the ones of NH_4^+, the preferred N form of the studied trees. Hence, the tree-ring $\delta^{15}N$ values reflect specific soil N conditions and assimilation modes by trees. Along with a wide tree-ring $\delta^{15}N$ range, we report differences in: soil nutrient content and N transformation rates; $\delta^{15}N$ values of NH_4^+, total dissolved N (TDN) and EcM mantle enveloping the root tips; and bacterial and fungal community structures. We combine EcM mantle and root $\delta^{15}N$ values with fungal identification to infer that hydrophobic EcM fungi transfer N from the dissolved organic N (DON) pool to roots under acidic conditions, and hydrophilic EcM fungi transfer various N forms to roots, which also assimilate N directly under less acidic conditions. Despite the complexities of

* Corresponding author.
E-mail address: martinem.savard@canada.ca (M.M. Savard).

https://doi.org/10.1016/j.scitotenv.2021.146581

soil biogeochemical properties and processes identified in the studied sites, in the end, the tree-ring $\delta^{15}N$ averages inversely correlate with soil pH and anthropogenic N inputs, confirming white spruce tree-ring $\delta^{15}N$ values as a suitable indicator for environmental research on forest N cycling.

1. Introduction

The release in the atmosphere of reactive N (NH_3, NH_4^+, NO, NO_2^-, HNO_3, NO_3^-) by human activities have more than doubled globally since the beginning of industrialization (Geng et al., 2014). These emissions along with co-pollutants may change air quality, modify climate dynamics by contributing greenhouse gases, and lead to acidification and eutrophication harming aquatic and terrestrial ecosystems. Understanding the specific effects of enhanced N on forest ecosystems rely on using natural archives such as tree-ring $\delta^{15}N$ values (e.g., Gerhart and McLauchlan, 2014). Given that most stem N loads in non-N_2 assimilating trees come dominantly from the root uptake of soil compounds, validating the role of tree-ring $\delta^{15}N$ values as an environmental indicator requires identifying the parameters that control the signals of the assimilated soil N forms and the fractionation steps leading to the final tree-ring $\delta^{15}N$ values (Savard and Siegwolf, 2021).

Trees can take up N compounds from soils through their roots, either directly (Näsholm et al., 2009; Averill and Finzi, 2011), or indirectly through the symbiotic association with EcM fungi (Näsholm et al., 2009; Courty et al., 2010; Lilleskov et al., 2019). Whereas the direct uptake of N minimally fractionates N isotopes, transfer through EcM fungi generates low $\delta^{15}N$ values in trees (Gebauer and Taylor, 1999; Hobbie and Hogberg, 2012). The N compounds available to trees and EcM fungi in soils, namely NH_4^+ and NO_3^- (dissolved inorganic N, DIN) and dissolved organic N (DON, dominant in total dissolved N, TDN), differ in their $\delta^{15}N$ values, and their separate analyses are difficult (Handley et al., 1998). Therefore, individual NH_4^+, NO_3^- and DON isotopic characteristics seldom appear in the literature. Moreover, N inputs in soils may change the $\delta^{15}N$ values of DIN (Mayor et al., 2014). Some studies report that anthropogenic N deposition near urban centers correlates with a decreasing $\delta^{15}N$ gradient of total N (TN) in subtropical soils (Kuang et al., 2011), and that separate $\delta^{15}N$ analyses of NH_4^+ and NO_3^- show the influence of traffic-derived NO_3^- on near-road mosses (Xu et al., 2019). Conceivably, tree-ring $\delta^{15}N$ values could also record pollution signals if the deposition of anthropogenic N modifies the $\delta^{15}N$ values of surface soil DIN.

The links between N assimilation through EcM fungi and $\delta^{15}N$ records in trees were mostly assessed in leaves (Hobbie et al., 2005; Craine et al., 2009; Mayor et al., 2012), and the impact of anthropogenic N on these links were generally examined in controlled experiments using very high N deposition (Högberg et al., 2011). However, chronic moderate anthropogenic N emissions are being deposited on N-limited forests covering extensive regions (e.g., McLauchlan and Craine, 2012), where the impacts of such inputs require retrospective assessments. The links between N assimilation through EcM fungi and tree-ring $\delta^{15}N$ values need to be evaluated for trees growing in field conditions, without experimental intervention, and under moderate anthropogenic N inputs.

As to the meaning of tree-ring $\delta^{15}N$ values, on one hand, studies suggest that they may not constitute faithful records of environmental conditions because their $\delta^{15}N$ trends depart from series in dated leaves that pick up airborne N (Tomlinson et al., 2015), do not correlate with leached NO_3^- from saturated soils as measured in stream water (Burnham et al., 2019), and seem marginally influenced by anthropogenic N deposition (Guerrieri et al., 2020). On the other hand, several studies interpret tree-ring $\delta^{15}N$ trends in terms of changes in N availability and environmental conditions due to the influence of anthropogenic N (McLauchlan et al., 2007; Savard et al., 2009; McLauchlan et al., 2017; Mathias and Thomas, 2018; Succarie et al., 2020), without assessing its impact on soil N components or knowing the $\delta^{15}N$ signals of deposited N (references in Gerhart and McLauchlan, 2014). In addition, the tree-ring $\delta^{15}N$ responses to N inputs are reported to be species-specific (Templer and Dawson, 2004; Islam and Macdonald, 2009; McLauchlan and Craine, 2012). Hence, tree-ring $\delta^{15}N$ values represent a needed indicator for forest N perturbations, but their significance is not straightforward. Our premise is that understanding the meaning of tree-ring values require looking at soil processes behind the root assimilation of N by individual tree species.

With the impetus of assessing the various controls on the final tree-ring $\delta^{15}N$ values, we conducted a detailed isotopic examination of stem rings and co-occurring roots in white spruce trees (*Picea glauca* (Moench) Voss), EcM mantles and soil N compounds to quantify the isotopic differences between soil N and roots and evaluate the fractionation steps in the soil-to-tree continuum. We sampled five stands of N-limited boreal forests exposed to moderate airborne anthropogenic emissions of variable amounts and isotopic signals. We characterized the soil chemistry and microbial communities near the selected trees to help pinpoint the factors controlling the fractionation steps. Our objectives were to: (1) find out if DIN in soil exposed to moderate anthropogenic N inputs reflects the anthropogenic N signals; (2) determine if the soil biogeochemical N dynamics differ among the five exposed sites; and (3) evaluate whether tree-ring $\delta^{15}N$ values directly reflect anthropogenic N signals or reflect responses to soil properties modified by anthropogenic pollution. Our working hypothesis was that soil conditions influenced by anthropogenic emissions modify the microbial communities, which in turn govern the fractionation of soil N before its assimilation by trees.

2. Materials and methods

2.1. Features of the sampling sites

Most Canadian provinces have maintained their N emissions stable for the last 25 years, therefore we opted to conduct this research in the province of Alberta (Canada) where N emissions are increasing. We selected sites in the N-limited forests of the two sectors recognized as the main causes for this increase: the lower Athabasca open-mining oil sands (OS) region near Fort McMurray, and the Edmonton region where coal-fired-power plants (CFPP) are still active (Fig. 1).

The lower Athabasca OS region is a wide emitter of diffuse contaminants, whereas the Edmonton CFPP region is impacted by intense emissions from the main point sources. We selected five sites to take into account various soil conditions and different anthropogenic inputs (Fig. 1). According to ground-verified modeling of emissions between 2011 and 2013, sites 2, V and C received 4.8, 4.1 and 3.9 kg/ha/y, while sites P and W received 6.0 and 8.1 kg/ha/y, at their specific grid points (Makar et al., 2018). These depositional rates significantly surpass the estimated background of 1 kg/ha/y (Fenn et al., 2015). Based on openfield wet samples collected at distances between 3 and 113 km from the main OS operations, the mean NH_4^+ and NO_3^- $\delta^{15}N$ values for summer were −0.4 and −4.0‰, respectively (Proemse et al., 2013), for a mean of −2.2‰ considering equal contributions from NH_4^+ and NO_3^-. Note that higher $\delta^{15}N$ signals were reported for DIN samples collected near the main OS emission zone (Proemse et al., 2013; Hemsley et al., 2019), but samples collected outside that zone tended to show lower means due to atmospheric processes (Proemse et al., 2013). Based on conditional sector samplers operating simultaneous collections of N forms emitted from the three CFPP, at distances

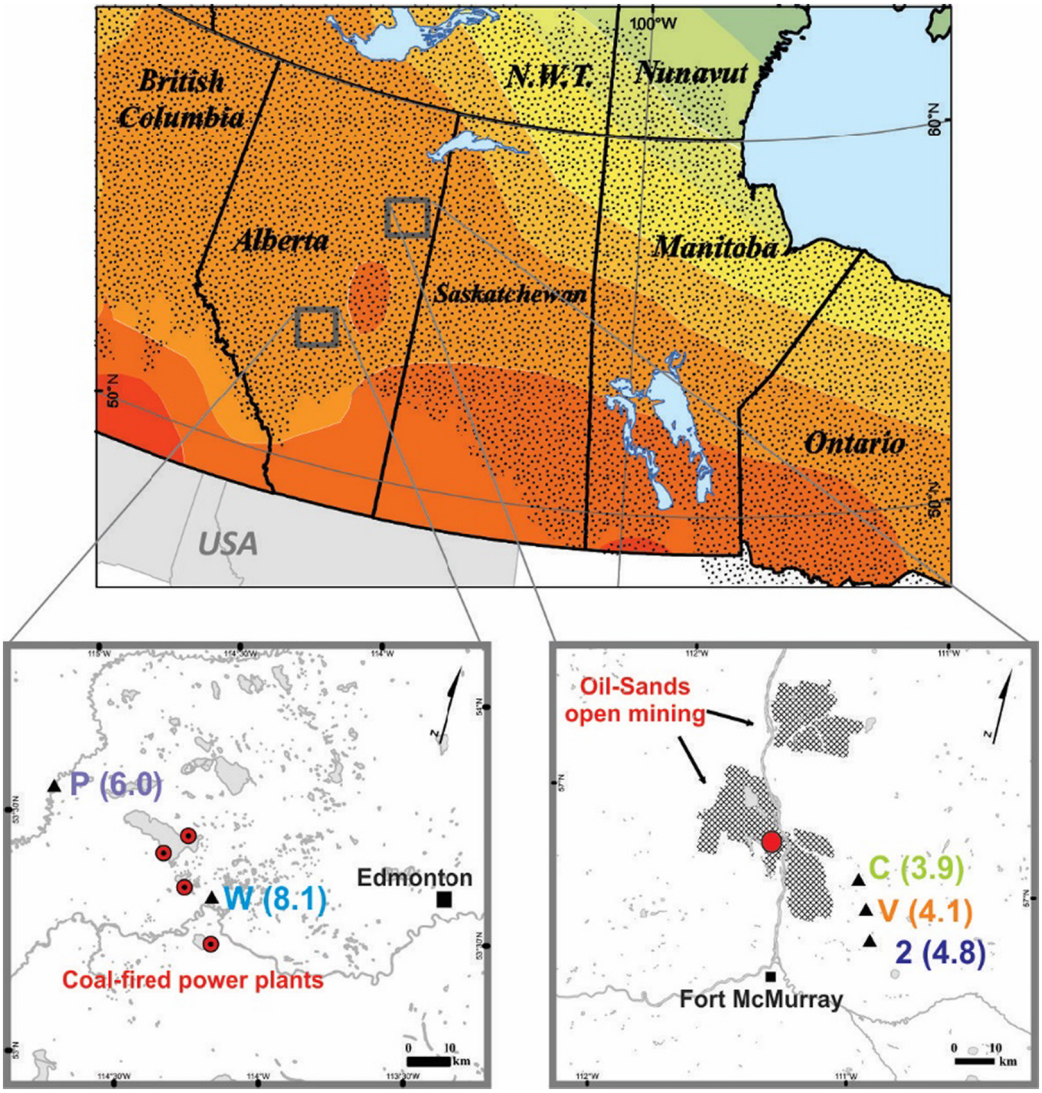

Fig. 1. Locations of the studied sites (triangles with colored labels) in the two regions of Alberta (after Savard et al., 2020a, 2020b). The red circles with dots in the lower left panel show the position of the coal-fired power plants (CFPP), west of Edmonton, and the red circle in the lower right panel, the geographic central point of the main oil sands (OS) open mining operations (shaded area) north of Fort McMurray. Numbers in parentheses are anthropogenic N inputs in kg/ha/y. The dotted area of the upper map shows the distribution of the boreal forest, and the colored surfaces reflect average summer-temperature zones (12–14 °C for the investigated areas). (For interpretation of the references to color in this figure legend, the reader is referred to the web version of this article.)

between 7 and 25 km, the particulate $\delta^{15}N$ means for the warm period were +11‰ for NH_4, and +4.9‰ for NO_3^- (Savard et al., 2017), giving a mean of +8‰ if both forms equally contributed to the deposition. The mean NH_4^+ and NO_3^- values were +1 and −1.2‰ if wet samples were included in the calculation (overall mean of 0‰). The diffuse emissions from the OS region were therefore depositing lower amounts of N contaminants with lower $\delta^{15}N$ values at the three selected sites relative to the two sites near the CFPP point sources of the Edmonton area.

The OS and CFPP regions have seen similar climatic conditions over the last decades. Over the 2013–2017 period, the summer rainfall was 189.1 and 200.2 mm for the OS and CFPP regions respectively, and summer temperature was 17.0 and 16.8 °C, in the same order (data from Fort McMurray and Stony Plain weather stations).

We sampled sites 2, V and C in the OS region, which were only accesssible by helicopter, and sites P (near Pembina River) and W (on the western slope of the Wabamun Creek valley) in the CFPP region, at walking distance from rural roads (Fig. 1) during fall, between 2013 and 2017. We chose the sites on the basis of similar white spruce health and status, and on soil drainage conditions to minimize the influence of such site conditions on soil microbial communities, N availability and assimilation modes by trees. Three dominant and mature trees (at least 92 years old), were selected at each site. All selected trees were established on well drained soils and showed no signs of damage or disease (see Section 2.2.1).

Site V in the OS region burned down during a large wildfire in the Fort McMurray in 2016. Consequently, three trees were sampled at this site, but soil and root samples were only collected around a single tree. These partial results complete the dataset of site C, which had similar soil conditions.

2.2. Field sampling

2.2.1. Soil samples

The soil characteristics from the two investigated regions showed many similarities mainly because they were formed under the same climatic conditions and, in many cases, on the same parent material (i.e., glacio-lacustrine deposits). In the OS region, the soils in sites V and C were almost the same and classified as Brunisolic Gray Luvisol (Canadian Society of Soil Science, 2020). In each site, the soil derived from a thin sandy eolian mantle overlying a loamy or clayey dominated glacio-lacustrine material. Both sites were well to moderately well drained and their mean pH values for organic horizons (FH; F-

fermentation and H-humified horizons) are 5.0 and 4.7 for site V and C, respectively. The soil conditions at site 2 were slightly different: Brunisolic soils were developed on well-drained sandy alluvial sands overlying coarse-grained glacio-fluvial material. At this site, the pH values for organic horizons varied from 4.2 to 6.9, with a high mean of 5.7 considering all investigated soil profiles (n = 4).

In the CFPP region, site P is located on a thick and compact loamy glacio-lacustrine deposit. Soils were typically (Orthic) Gray Luvisol and despite the nature of their parent material, site P soils were considered moderately well drained. The mean pH value for the organic horizons was 6.0. The site W is located on deposits consisting of fine alluvial sands overlying loamy dominated glacio-lacustrine material locally affected by slope movements (colluvium). In general, the conditions were suitable for the development of brunisolic soils even if Regosols were observed at unstable places. Irregular topography along the slope leads to variable drainage conditions from moderately well drained to imperfectly drained. Finally, the mean pH value for organic horizons was 5.6.

Soil samples from the organic layers (F and H) and the mineral soil horizons (A-eluvial and B-illuvial) were collected in the north, south, east and west directions, in the immediate surroundings (~2 m radius) of each selected tree at all sites (FHAB sample set). In addition, pedons (complete soil profiles) were sampled. Samples were sieved at 4 mm for organic, and 2 mm for mineral horizons. The FHAB horizons near trees were split into three parts for the different analytical treatments: $\delta^{15}N$ analyses, microbial and biogeochemical characterizations. For the latter, samples were refrigerated, whereas those collected for $\delta^{15}N$ analyses and molecular characterization of microbial communities were immediately frozen in dry ice and kept frozen until lyophilization in the laboratory. In addition, two to three pedons were dug to describe the pedogenetic conditions at each site and samples of the L, F, H, A, B and C horizons were collected and immediately frozen for the analyses of $\delta^{15}N$ values.

2.2.2. Rootlets, EcM mantles and tree rings

Rootlets along with their EcM mantles were collected at each cardinal point around the trees selected for isotopic analyses. Samples were stored in brown paper bags to let them dry naturally. In the laboratory, rootlets and EcM mantles were air dried and separated into two equal parts for the isotopic and microbiome studies (EcM fungi from root tips; Section 2.3.3).

Stem sections collected at breast height of three mature trees selected at each site were let to dry out prior to subsampling for the isotopic analytical work. Four radii of the tree stems were cut apart in four perpendicular directions. Once dated and measured for their width, the rings from each radius were dissected into individual growth rings and combined into a given-year sample using equal weights.

2.3. Preparation protocols and analyses in laboratories

2.3.1. Isotopic analyses of the various matrices

All treatment and isotopic analyses were performed at the Delta-Lab of the Geological Survey of Canada (Québec, QC). For the isotopic analyses of N compounds, the frozen FHAB and pedon samples were lyophilized, sifted, ground and homogenized. The FHAB samples from the four cardinal points were combined for each tree, and used for the characterization of DIN and DON (protocols in Fig. A.2.1).

For all soil N forms, we opted for the elution from samples using water with a pH of 5.2 representative of Alberta rain to reproduce the natural bioavailability of N components in soils. In order to proceed with the isotopic characterization of soil samples, NH_4^+ and NO_3^- + NO_2 concentrations in the organic horizons were determined using the LACHAT Autoanalyser, and in the inorganic horizons, using an ion chromatograph (Integrion, ThermoFisher Scientific) at Institut national de la recherche scientifique (INRS), centre Eau-Terre-Environnement (ETE). The preparation protocols for the analyses of soil NH_4^+, NO_3^- and TDN required large amounts of material due to the low concentrations of DIN in soils. Afterwards, the samples were centrifuged and filtered. In some cases, the amount of eluted material was not sufficient for retreatment or duplication of the samples. Consequently, the three compounds, especially those of low concentration in the A and B horizons (NH_4^+ and NO_3^-), could not be measured in all the samples. The NH_4^+ ions were then separated using the diffusion method (e.g., Sebilo et al., 2004; Hannon and Böhlke, 2008), and trapped as ammonium citrate ($C_6H_{11}NO_7$) on glass fibre filters previously acidified with citric acid (Schleppi et al., 2006), and dried in a desiccator. These treated samples were analyzed using an elemental analyzer online with an isotope ratio mass spectrometry (EA-IRMS; Costech attached to a Delta V; Thermo Fisher Scientific). The precision of the full preparation and analytical protocols was 0.4‰, based on repeats of several samples. The NO_3^- ions were extracted following the chemical method including Cd for reducing nitrate into nitrite, and sodium azide to produce nitrous oxide (N_2O; Smirnoff et al., 2012). Through the period of investigation, we assessed the efficiency of the column on numerous nitrate standards. The produced N_2O was analyzed using a pre-concentrator with gold furnace online with an IRMS (Au-PreCon Delta V), which produces $\delta^{15}N$ results on N_2, avoiding the need to correct for the ^{17}O contribution on m/z = 45 as required with the regular N_2O method. The precision of the method was 0.7‰. A sub-sample of lyophilized, centrifuged and filtered soil material served for TDN determination using the EA-IRMS system. The precision of this method was 0.2‰. A mass balance calculation using the proportions and $\delta^{15}N$ values of the TDN and DIN (e.g., Liu et al., 2013) helped determine the final $\delta^{15}N$ values of the DON (precision 0.2‰; Fig. A.2.1). Owing to the dominance of DON in TDN (Mayor et al., 2015), we use the TDN $\delta^{15}N$ results as a proxy for DON values.

Samples of rootlets coated with EcM mantles collected at each cardinal point around the trees were split in half to perform the isotopic and microbiome analyses. For the isotopic analysis, the samples from each cardinal point around a tree were combined in order to obtain enough material for the analytical protocols. The combined samples were placed in test tubes containing ethanol and sonic bathed to detach the fungal material from rootlets. The root tips (free of fungal mantle) were recovered from the test tubes while the detached soft fungal material (mantle around root tips) was dried out by evaporation of the solvent.

The preparation of tree-ring wood and rootlets for isotopic analysis followed the protocol presented in Savard et al., 2020b. Briefly, the post-subsampling methodology included grinding all combined whole-wood tree-ring samples for individual analyses. For the purpose of following the soil to stem isotopic path, we report here the mean for the last five years of the collected sections. Note that using the last year value, or the mean for 2 or 10 years gave similar departures between trees and sites. All rootlets, EcM mantle and tree rings were analyzed with the EA-CF-IRMS system, at a precision of 0.3‰ or better, based on repeats of several samples.

2.3.2. Soil chemical analyses and incubations

All chemical analyses of soil samples were performed at the Forest Soils Lab of the Laurentian Forestry Centre (NRCan-CFS-LFC). The pH of soil samples was measured in a 0.01 M $CaCl_2$ solution (Carter and Gregorich, 2007). Exchangeable cations (as cmol+/kg) and extractable phosphorus (P; mg/kg) were determined by ICP-OES (Optima 7300 DV, Perkin Elmer, Waltham, MA, USA) following a Mehlich III extraction. The cation exchange capacity (CEC) was calculated as the sum of exchangeable cations in equivalent (Eq) unit (Carter and Gregorich, 2007). The basic cation saturation ratio (BSCR) was calculated as equivalent (Eq) units ((potassium (K) + sodium (Na) + calcium (Ca) + magnesium (Mg)) / CEC) * 100 (e.g., Thiffault et al., 2006). In the following text, cations (K, Ca, Mg, Mn and Na) designate exchangeable elements in Eq unit, and P designates extractable phosphorus in concentration unit.

The NH_4^+-N and NO_3^--N (mg/kg) were extracted with a 2 M KCl solution and analyzed by spectrophotometry (QuikChem R8500 Series 2, Lachat Instruments, Loveland, CO, USA). The DON (g/kg) was analyzed on the same samples following oxidation of a subsample with K-persulfate ($K_2S_2O_8$) and boric acid (H_3BO_4) at 121 °C and 135 kPa in an autoclave which oxidizes all N forms to NO_3^- (Cabrera and Beare, 1993; Carter and Gregorich, 2007). Net mineralization (μg NH_4^+-N/kg/d) and net nitrification (μg NO_3^--N/kg/d) were assessed by incubating soil samples under laboratory conditions in the dark for 42 days and comparing pre- and post-incubation values (Gauthray-Guyénet et al., 2018). Total C and N concentrations (%) were determined by dry combustion using a TruMac CNS analyzer (LECO Corporation, St. Joseph, MI, USA).

2.3.3. Molecular characterization of soil microbial communities

Soil bacterial and fungal communities from the F and H horizons and from the EcM root tips were characterized using targeted amplicon sequencing of bacterial and fungal phylogenetic marker genes (Stefani et al., 2018). Briefly, genomic DNA was recovered from 150 mg of soil from the F and H horizons or 50 to 100 mg of ground root tips using the DNeasy PowerSoil kit (Qiagen, Valencia, CA, USA). The bacterial V4–V5 16S rRNA gene and the fungal internal transcribed spacer 2 (ITS2) region were then amplified the primer sets 341F/805R (Herlemann et al., 2011) and ITS3_KYO2/ITS4 (Toju et al., 2012). Library preparation and sequencing on an Illumina MiSeq platform was performed as recommended by the manufacturer for user-defined primers (Illumina, 2013).

All bioinformatics analyses were performed in QIIME (version 1.9.1; Caporaso et al., 2010). Briefly, sequence reads were merged with their overlapping paired-end (fastq_mergepairs), trimmed to remove primers (fastx_truncate), and filtered for quality (fastq_filter; expected error threshold (fastq_maxee) set to 1) using USEARCH (Edgar, 2010). Unique identifiers were inserted into the header of the remaining high-quality sequences, and sequences from the different samples were pooled together (add_qiime_labels) prior to further analyses. UPARSE (Edgar, 2013) was then used to dereplicate the sequences (derep_fulllength), discard singletons (sortbysize), group high quality reads into operational taxonomic units (OTUs) using a 97% identity threshold (cluster_otus; Schloss et al., 2009), and identify chimeras (_ref). The taxonomic assignment of OTUs was performed with the command "assign_taxonomy" as implemented in QIIME using Greengenes database (McDonald et al., 2012) and the UNITE database (Abarenkov et al., 2010), for bacteria and fungi, respectively. The command "*make_OTU_table*" was then executed to produce the OTU tables in the "biom" format. The 16S OTUs assigned to chloroplasts, mitochondria and to the kingdom *Plantae* and the ITS2 OTUs assigned to the kingdoms *Protozoa*, *Protista*, *Chromista* and *Plantae* were removed using the command "filter_taxa_from_otu_table". Using the same command, rare OTUs in OTUtables (relative abundances ≤0.005%, Bokulich et al., 2013) were removed. Each sample was rarefied to the lowest number of reads observed in libraries for each dataset (command "*single_rarefaction*"). The rarefied OTU tables were used for downstream analyses. Ecological guild for each fungal OTU was obtained using FUNGuild (Nguyen et al., 2016). Only guild assignments with a "probable" or "highly probable" confidence ranking were considered.

2.3.4. Statistical analyses

Statistical relationships between N deposition, soil properties and $\delta^{15}N$ values were performed using the Excel Pearson function on correlation matrices. Multivariate statistical analyses for the microbiome were performed in R version 3.5.3 (R-Core-Team, 2019) with the R package *vegan* v2.5-6 (Oksanen et al., 2007), unless stated otherwise. The OTU table of the EcM community recovered from the root-tip sequencing was converted into presence/absence with the "*decostand*" function and analyzed using a modified Raup–Crick dissimilarity matrix (Chase et al., 2011). The EcM status of the OTUs was confirmed with FUNGuild. For the soil samples, Bray-Curtis distance based on bacterial or fungal OTU relative abundance was calculated with the function "vegdist". The relationships between the structure of soil microbiome and the environmental variables measured in the F and H horizons (pH, P, Mn, Mg, K, Na, Ca, BCSR, Total N, NO_3, NH_4, C/N ratio, nitrification, mineralization) were visualized with distance-based redundancy analysis (db-RDA) using the function "*dbrda*". The best environmental predictors were identified following a stepwise selection, as previously described (Blanchet et al., 2008). Highly correlated covariables were removed based on variance inflation factors (VIF) to avoid multicollinearity, using the function "*vif.cca*". Variables having a VIF > 10 were removed from the analysis until all remaining variables had a VIF < 10 (Hair, 2011). Then, a backward and a forward selection were used to eliminate the variables that explained no significant variation ($p > 0.05$) using the function "ordistep". This allowed to find the best model for the calculation of the db-RDA. The ordination analysis outputs were visualized using the R package *ggplot2* v3.3.2 (Wickhame, 2016). The same approach was used to assess the relationships between EcM fungi colonizing the tree root tips and the environmental variables or the tree-ring $\delta^{15}N$ averages. Spearman correlation analyses were performed using the function "*corr.test*" (R package psych v2.0.9 (Revelle, 2020) to determine if the soil pH was correlated with the alpha-diversity indices of bacterial and fungal communities. Alpha-diversity indices (Shannon index, Simpson's index and Richness, defined as the number of OTUs) were calculated using the function "diversity".

3. Results

3.1. The $\delta^{15}N$ values of soil N compounds and tree rings

To pinpoint the key drivers behind the tree-ring $\delta^{15}N$ changes, we first display and interpret the soil and tree-ring $\delta^{15}N$ differences per region (Fig. 2). Then, we explore the potential influences of soil properties on EcM $\delta^{15}N$ values and on the tree-ring $\delta^{15}N$ results at the tree level (Fig. 3).

The DON (n = 12) extracted using the two preparation protocols dominate the TDN (n = 20) (Tables A.1.1, A.1.3), as previously documented (Mayor et al., 2015). Moreover, the DON $\delta^{15}N$ values in the F horizons are slightly lower than the ones of TDN, however in the H horizons or in combined F and H horizons, they are always slightly heavier (Table A.1.3). Therefore, TDN $\delta^{15}N$ results can be used as proxy for DON values. The mean TDN $\delta^{15}N$ values in the organic horizons near trees and in pedons of the OS sites range between +2.4 and + 4.7‰, and are systematically higher than the TDN $\delta^{15}N$ values in the CFPP region that vary between −2.0 and +0.6‰ (Fig. 2A). Interestingly, the organic horizons of the two regions show separate, but similar positive trends between NH_4^+ and TDN $\delta^{15}N$ results (Fig. 2A). Most points of the dataset show positive $\delta^{15}N$ differences (substrate minus product) between TDN (assumed substrate) and NH_4^+ (product), except for two points that belong to site P from the CFPP region (highest grey squares on Fig. 2A; or Fig. A.3.2A). The mean NO_3^- $\delta^{15}N$ values as a function of TDN $\delta^{15}N$ results in the organic horizons show no trends, but very distinct groupings for the two regions (Fig. 2B); the OS region showing much lower NO_3^- values (−10.3 to −5.6‰) than the CFPP samples (+1.6 to +5.0‰).

Despite the fact that the data were from a single tree species, the tree-ring $\delta^{15}N$ means varied widely across sites, from −3.2 to −0.9‰, and inversely correlated with pH means (Fig. 2C). The two lowest pH means per site for the organic horizons belong to sites with the lowest anthropogenic N inputs, in the OS region (Fig. 2D). The highest pH means (>5.5), either from the OS or CFPP regions, corresponded to the highest N deposition. In the OS region, this relationship forms a three-point line on which site 2 showed the highest N deposition and pH values (upper yellow circle). The P and W sites from the CFPP region with high pH did not line up with the OS trend, but if the fives sites were considered, a positive correlation still existed (Fig. 2D). The highest pH

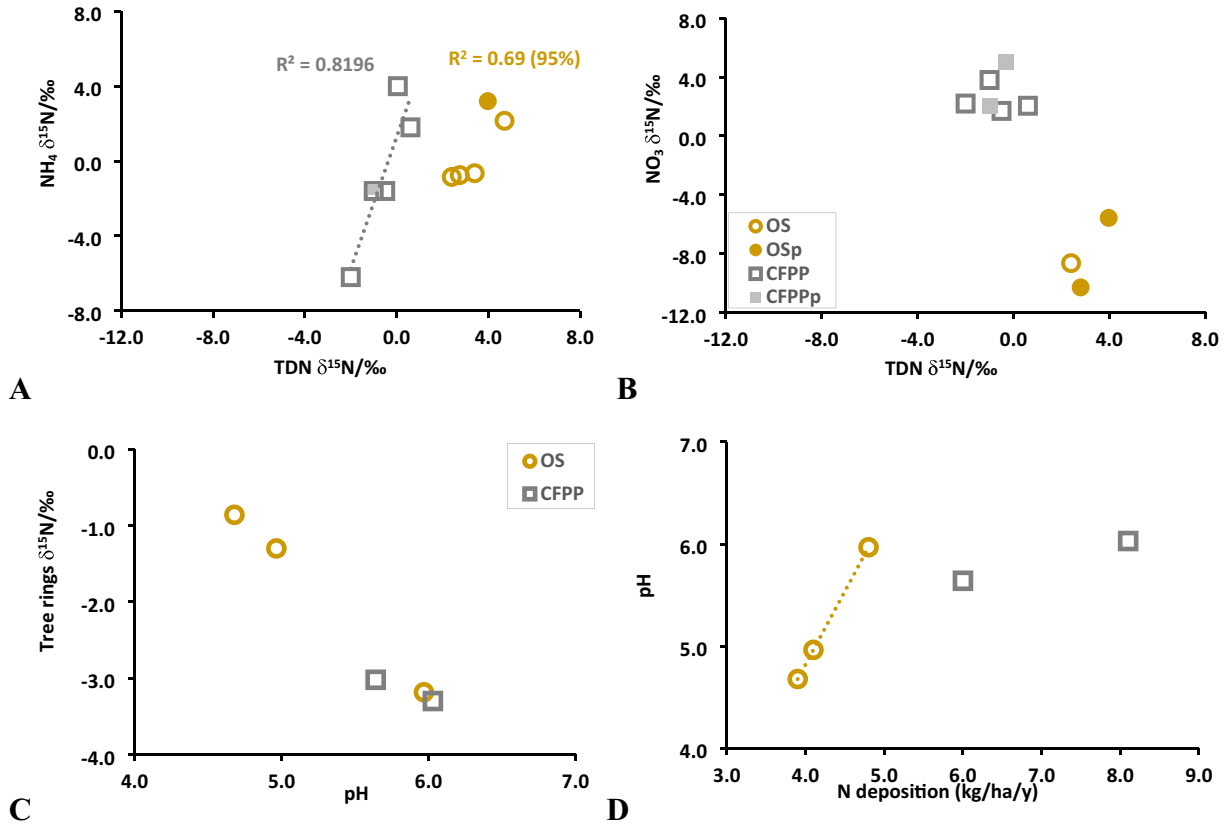

Fig. 2. Average results per site in the OS and CFPP regions. The NH_4^+ (A) and NO_3^- (B) $\delta^{15}N$ values as a function of TDN $\delta^{15}N$ values in the F and H soil horizons. The horizontal dotted lines show the upper and lower limits of the $\delta^{15}N$ averages for the airborne DIN: ochre in the OS region, grey in the CFPP region (Section 2.1). Tree-ring $\delta^{15}N$ means as a function of pH of F and H horizons (C), and pH as a function of the anthropogenic N deposition (D). Legend in B stands for all sites (p subscripts for *pedon* indicated by full symbols; open symbols for near-tree samples). Dotted correlation lines for individual regions according to mentioned color code, solid lines, for the full data set.

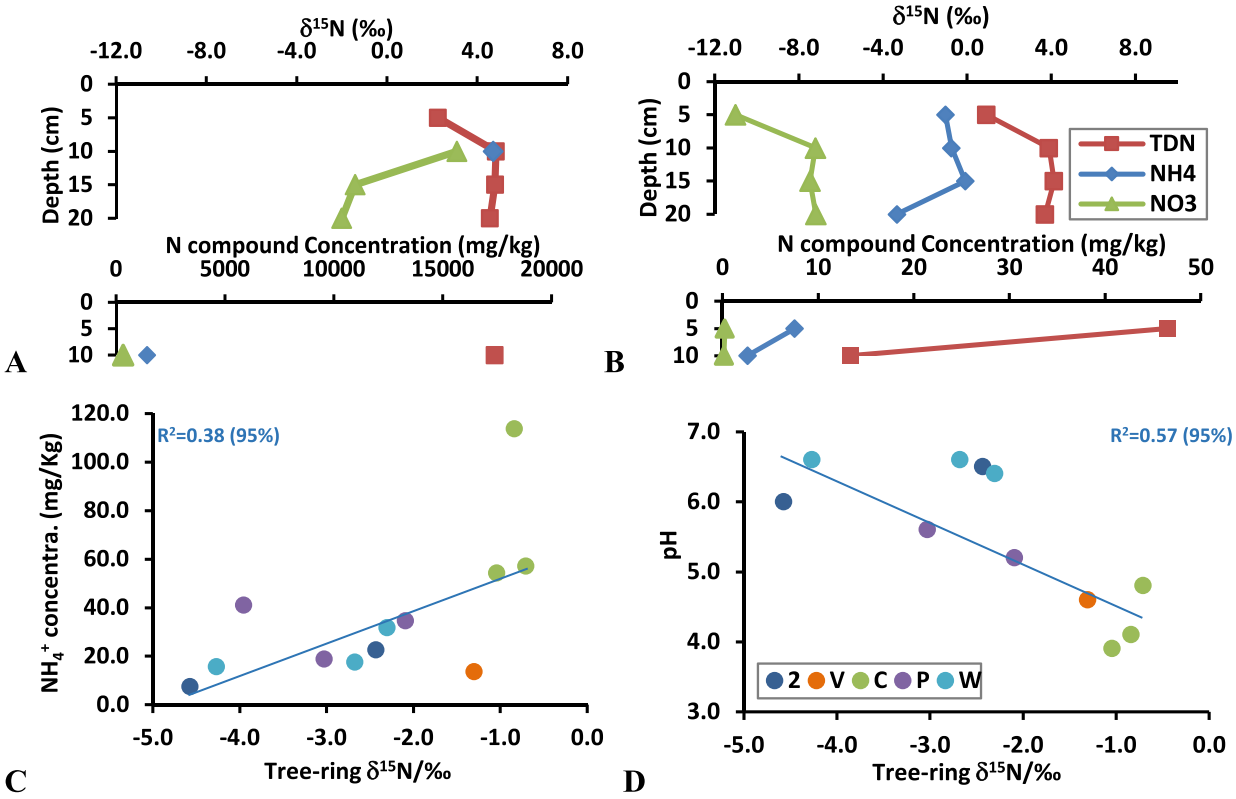

Fig. 3. Results per tree. Examples of sites 2 (tree 2-21; A) and C (tree C-3; B) showing $\delta^{15}N$ values (upper panels) and concentrations (lower panels) obtained for TDN, NH_4^+ and NO_3^- in the F, H, A, and B soil horizons (in descending order). Legend in B stand for graph in A as well. The F and H NH_4^+ concentration (C) and mean F, H, A, B pH (D) as a function of the tree-ring $\delta^{15}N$ values. Legend in D stands for graph in C. Numbers in parenthesis represent the correlation confidence level.

mean at site P corresponds to the highest anthropogenic N input. The lowest anthropogenic N inputs and soil pH correspond to the highest $\delta^{15}N$ results in trees (Fig. 2C, D).

The soil N compounds near trees showed variable relationships in the F and H horizons, but the TDN (DON) concentrations were generally higher than the NH_4^+ and NO_3^- ones (Table A.1.3; Fig. 3A, B). The general FHAB isotopic profiles depicted high $\delta^{15}N$ values in TDN and DON, intermediate values in NH_4^+ and low ones in NO_3^- (Fig. 3A, B; Figs. A.4.2, A.4.3).

The concentration of NH_4^+ in the soil organic horizons correlated positively with the tree-ring $\delta^{15}N$ values, whereas pH of the F, H, A, and B soil layers correlated inversely (Fig. 3C, D). The F and H horizons of sites C and V were generally more acidic than the other sites of the two regions (Fig. 3D).

3.2. The $\delta^{15}N$ values from soils to EcM mantles, rootlets and tree rings

In this section, we track the $\delta^{15}N$ results from soil N compounds to EcM mantles, roots and rings at the tree level, examine their links (Table 2), then we interpret the $^{15}N/^{14}N$ fractionation between EcM mantle and tree rings.

As established above, NH_4^+, the preferred DIN form of white spruce trees, mostly derives from DON which represents an important portion of TDN (Table A.1.3). We noted that the TDN $\delta^{15}N$ signals of the investigated trees strongly correlate with the mean mantle $\delta^{15}N$ values (Table 2). Examining the specific TDN-mantle $\delta^{15}N$ distribution per site, we observed a direct correlation, and a clear grouping of the site C (OS) results on the heavy end of the range; the CFPP sites (P, W) showed wider $\delta^{15}N$ arrays (Fig. 4A). We also noted that the soil NH_4^+ and mantle $\delta^{15}N$ values did not define a straight pattern, and that site C results clustered on the heavy end of the EcM $\delta^{15}N$ range, but with relatively low NH_4^+ values (Fig. 4B). The EcM mantle $\delta^{15}N$ values correlated negatively with pH, positively with NH_4^+ concentration and $\delta^{15}N$ values, and to a lower extent, negatively with the net nitrification and mineralization (only in H) rates (Fig. 4B, Table 1).

Table 1
Correlations (Pearson) between the EcM (mantle) $\delta^{15}N$ results per tree and means of potential controlling parameters in F and H soil properties (data in Table A.1.1).

Soil horizon	F	H	F&H
pH ($CaCl_2$)	−0.11 (7)	***−0.83*** *(6)*	***−0.70*** *(10)*
NH_4^+	0.61 (8)	−0.79 (6)	***0.69*** *(10)*
NO_3^-	−0.19 (8)	−0.64 (6)	−0.32 (10)
TDN	−0.41 (6)	**−1.00 (3)**	0.16 (7)
Mineralization	0.32 (8)	−0.73 (7)	0.22 (11)
Nitrification	−0.43 (8)	−0.74 (7)	−0.57 (11)

Bold coefficients for 99% confidence level, bold italic, for 98%, and underlined, for 95%. (n): number of paired variables.

The rootlet $\delta^{15}N$ results correlated with the mantle values (Table 2), and displayed lighter values relative to the mantle results (Fig. 4C). In other words, the paired rootlet-mantle $\delta^{15}N$ results fell to the right of the 1:1 relationship, harbouring a slope of 0.4, and an apparent strong isotopic fractionation by EcM mantle at site C (mean isotopic difference, i.e., $\Delta\delta^{15}N_{mantle\text{-}roots}$, of −4.6‰) relative to the other sites (means $\Delta\delta^{15}N_{mantle\text{-}roots}$ of −3.2 and −2.3‰ for W and P, respectively). The EcM mantle of several trees (sites V, P, and one tree at site W) had $\delta^{15}N$ values lower than the corresponding NH_4^+ results ($\Delta\delta^{15}N_{mantle\text{-}NH4}$ between −3.6 to −0.9‰), whereas the mantle from two trees at site W showed higher values ($\Delta\delta^{15}N_{mantle\text{-}NH4}$ of +0.6 and +5.0‰).

The rootlet and tree-ring $\delta^{15}N$ trend fell slightly below the 1:1 relationship (Fig. 4D). The highest tree-ring $\delta^{15}N$ cluster belonged to the trees from sites C and V; wider $\delta^{15}N$ ranges were observed for the other sites (2, P and W).

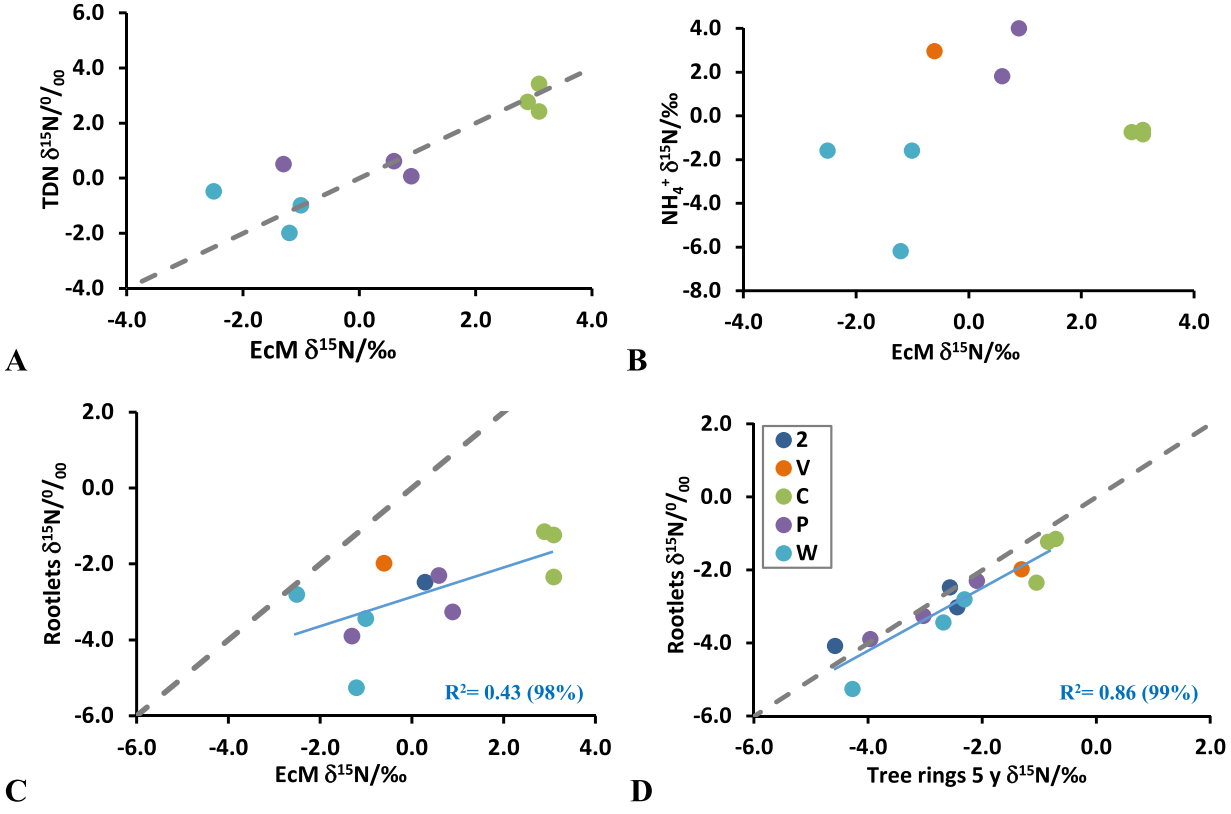

Fig. 4. Isotopic results for all studied trees. The TDN (A) and NH_4^+ $\delta^{15}N$ values in F and H horizons (B), and in rootlets (C) as a function of mantle EcM $\delta^{15}N$ values. Rootlet values as a function of the mean $\delta^{15}N$ values of the last five tree rings (D). Dashed lines indicate a 1:1 relationship. Note that results for several trees are missing because either soil or EcM values could not be measured due to insufficient quantities of the sampled material (see Section 2.2). Legend in D stands for all graphs.

Table 2
Correlations (Pearson) between the $\delta^{15}N$ values of soil N compounds from the F and H soil horizons per tree with the EcM mantles, root and tree-ring $\delta^{15}N$ values (5-year mean), and with the pH of the F, H, or F, H, A, B horizons (data in Table A.1.3).

$\delta^{15}N$	H-NO_3^-	H-NH_4^+	F&H NH_4^+	H-TDN	F&H TDN	EcM	Roots	5y TR
EcM	−0.39 (6)	−0.64 (6)	0.22 (10)	0.20 (7)	**0.87** (9)		***0.66*** *(11)*	**0.70** (11)
Roots	−0.38 (7)	−0.52 (8)	0.46 (10)	0.19 (9)	0.46 (11)			**0.93** (13)
pH FH	**0.88** *(6)*	0.42 (8)	−0.07 (10)	−0.21 (8)	−0.36 (10)	***−0.70*** *(9)*	−0.54 (11)	***−0.59*** *(11)*
pH FHAB	***0.82*** *(5)*	***0.79*** *(7)*	−0.21 (9)	0.06 (7)	−0.44 (10)	**−0.94** (8)	**−0.74** (10)	**−0.74** (10)

Bold coefficients for 99% confidence level, bold italic, for 98%. (n): number of paired variables.

3.3. Microbial communities

Here, using multivariate and univariate correlation approaches, we examine whether the dissimilarities in soil properties were associated with differences in bacterial and fungal communities, and with the presence of specific microbial taxa that could influence the soil N dynamics.

3.3.1. Links between soil properties and soil microbial communities

The db-RDA was first used to assess the links between soil properties and the overall structure of the bacterial and fungal communities. The db-RDA were significant ($p < 0.001$) for both soil bacterial (Fig. 5) and fungal communities (Fig. 6) in the F and H soil horizons. The environmental variables explained 54.2% and 67.1% of the total variation in the bacterial community composition in the F and H horizon, respectively (Fig. 5). For the fungal communities, the environmental variables explained 59.9% of the total variation in the F horizon (Fig. 6A) and 47.2% in the H horizon (Fig. 6B).

Soil pH best explained the structure of the bacterial community in the F and H horizons (Fig. 5) and of the fungal community in the F horizon (Fig. 6A). Overall, the soil pH was positively correlated ($p < 0.05$) with bacterial (F and H horizons) and fungal (F horizon) diversity indices (Table 3). Regarding the H horizon, the structure of the fungal community was driven by total N and Mg concentrations as these variables showed the strongest correlation with the first axis of the ordination (Fig. 6B). Phosphorus was the second most important variable driving the structure of bacterial and fungal communities of the F and H horizons (Figs. 5, 6). Total N was a significant driver only for the fungal community structure in both horizons (Fig. 6).

The db-RDA further identified several bacterial and fungal OTUs that significantly contributed to the dataset variation and were closely associated with the soil properties (grey and black arrows in Fig. 5; blue, brown, light green and dark green in Fig. 6). Interestingly, the relative abundance of several OTUs belonging to the phylum *Actinobacteria* (e.g., three OTUs assigned to the orders *Actinomycetales* and *Acidimicrobiales* in horizon F, and six in horizon H) was negatively correlated to the soil pH in both the F and H horizons (Fig. 5). A total of 14 bacterial taxa from various phyla, including taxa potentially involved in N fixation (e.g., *Rhodoplanes* and *Burkholderia* from the phylum *Proteobacteria* and *Pedobacter* from the phylum *Bacteroidetes*), had high relative abundances in soils from the P and W sites and in the H horizon from the P site (no H horizon at the W site) and were negatively correlated to the C/N ratios (Fig. 5).

Regarding the fungal community, the relative abundances of several OTUs assigned to the genera *Piloderma* and *Meliniomyces* and to the ecological EcM guild were high in sites C and V and positively correlated to total N (Fig. 6) for both the F and H horizons. Conversely, four OTUs assigned to the ecological guild of saprotrophs (brown arrows) had higher relative abundances at the P and W sites and were positively correlated to the soil pH (Fig. 6A). We further tested the correlation between soil pH and the alpha diversity indices deduced from metabarcoding data, and pH was identified as an important driver (Table 3).

3.3.2. Ectomycorrhizal communities associated with white spruce root tips

A total of 221 ectomycorrhizal OTUs were recorded. The db-RDA was significant ($p < 0.001$) and the selected environmental variables

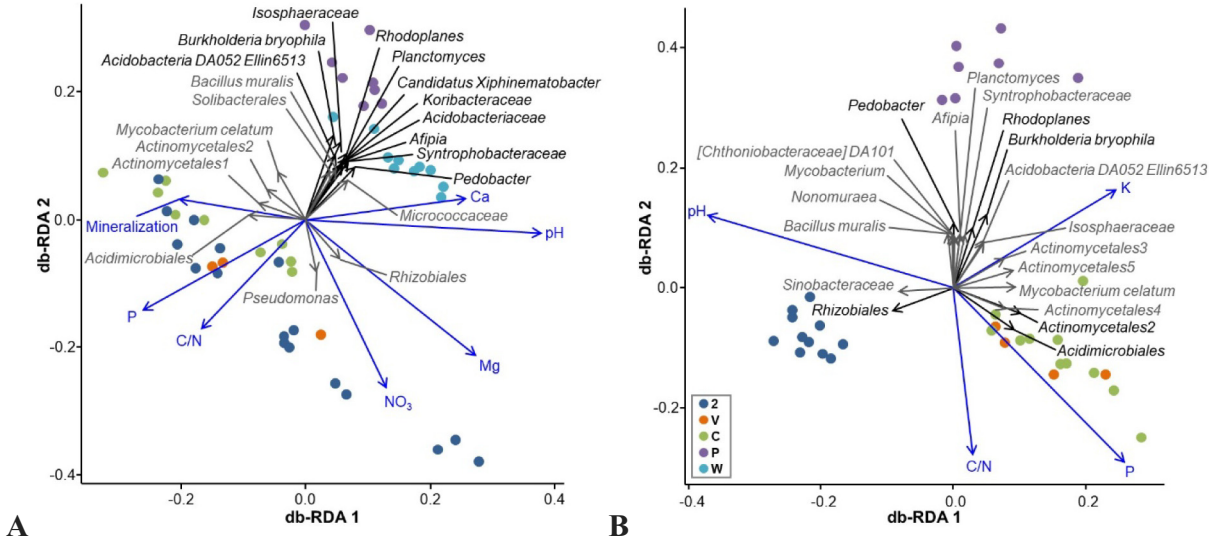

Fig. 5. Correlation triplots using distance-based redundancy analysis (db-RDA) of the variation in soil bacterial community data constrained by the soil properties in the F (A) and H (B) horizons. Grey and black arrows represent arrow lengths of <0.1 and ≥0.1, respectively. The following description stands also for Figs. 6 and 7; legend in B stands for the two graphs; points represent site ordination scores; blue arrows represent environmental variables scores; grey and black arrows represent OTUs scores; the graphs show the 20 most abundant OTUs among those having the highest contribution to the dataset variation (arrow length > 0.08); blue arrows are reduced to 40% of their length for scale; taxonomic identification of each OTU is provided at the lowest taxonomic level assigned. (For interpretation of the references to color in this figure legend, the reader is referred to the web version of this article.)

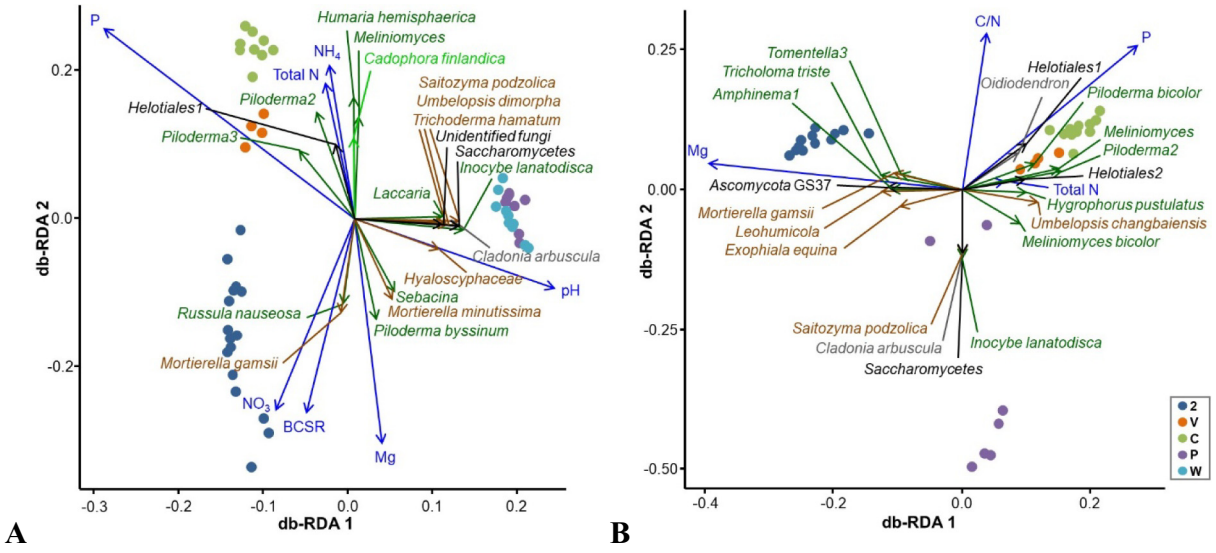

Fig. 6. Correlation triplots based on db-RDA using the soil fungal community data constrained by the soil properties in the F (A) and H (B) horizons. Note that we use total N as a proxy for TDN (correlation at R^2 of 0.50, 99% confidence level), because TDN values could not be produce for all samples. Fungal names and arrows are colored according to their ecological guild: ectomycorrhiza (dark green), endophytes (light green), saprotrophs (brown), other symbiotrophs (grey); undefined functions (black); see legend of Fig. 5 for more details. (For interpretation of the references to color in this figure legend, the reader is referred to the web version of this article.)

explained 63.4% of the total variation in the EcM structure (Fig. 7A). Soil pH was not a significant driver of the ectomycorrhizal community in root tips.

Soil K, Mn and NH_4 concentrations, C/N ratio and nitrification showed strong correlations with the first and second axes of the ordinations (Fig. 7A). Even if no clear grouping of samples according to sites was observed on the first axis of the ordination, EcM communities in root tips of sites C and V formed a distinct cluster and were correlated with high Mn and NH_4^+ concentrations (NH_4^+ was statistically linked with the mantle EcM $\delta^{15}N$ values; Section 3.1).

The db-RDA performed on pooled EcM OTU presence/absence data from each tree (species variable), using tree-ring $\delta^{15}N$ ratios as environmental variable was significant ($p = 0.03$; Fig. 7B), and the tree-ring $\delta^{15}N$ values explained 26.9% of the variation in the EcM community. High tree-ring $\delta^{15}N$ values detected at site C positively correlated with the relative abundances of two *Piloderma* OTUs (*Piloderma2*, *P. bicolor*), while they were negatively correlated with OTUs identified as *Tomentella1* and *Inocybe lanatodysca* (Fig. 7B).

4. Discussion

4.1. The limited influence of anthropogenic emissions on $\delta^{15}N$ values of soil N compounds

The OS sites had higher TDN $\delta^{15}N$ means than the CFPP sites, suggesting no influence from anthropogenic N inputs, which would have generated the opposite effect (Proemse et al., 2013; Savard et al., 2017). This finding was not surprising because TDN amounts in soils are large relative to those of DIN (Tables A.1.1, A.1.3), and their $\delta^{15}N$ values are mostly controlled by organic matter decomposition by various agents, litter contribution, and illuviation of N into deep soil layers (e.g., Nadelhoffer and Fry, 1988; Hobbie and Ouimette, 2009). When considering the distinct $\delta^{15}N$ signals of the industrial emissions in the OS and CFPP regions (see Section 2.1), our NH_4^+ $\delta^{15}N$ results were counterintuitive (Fig. 2A), because a cause-and-effect relationship with anthropogenic N signals would impart lower soil-N $\delta^{15}N$ values in the OS region relative to the CFPP area (colored squares; Fig. 2A). We observed similar maximal NH_4^+ $\delta^{15}N$ values in the two regions, but the CFPP sites averaged lower and the OS sites higher than their respective regional airborne signals (Fig. 2A). These observations indicate that the $\delta^{15}N$ signals of the anthropogenic N inputs do not regulate the $\delta^{15}N$ values of the soil NH_4^+. Anthropogenic N inputs not regulating the signals of NH_4^+, the preferred N form for white spruce trees, represents an informative finding, which forbids the application of the concept of signal transfer from pollutants to trees (Saurer et al., 2004, Bukata and Kyser, 2007, Savard et al., 2009, Härdtle et al., 2013; see Section 4.4).

The TDN and NH_4^+ $\delta^{15}N$ relationships indicate that, in both regions, ^{15}N-depleted NH_4^+ mostly derives from the mineralization of ^{15}N-rich DON (Fig. 2A), the major constituent of soil soluble N, as expected for microbial mediation of N transformations (e.g., Pardo and Nadelhoffer, 2010). The only exceptions to this rule are from site P, where the NH_4^+ might have been subjected to intense nitrification and consumption by roots and EcM fungi (McLauchlan and Craine, 2012). Such processes tend to increase the $\delta^{15}N$ values of residual NH_4^+; they likely explain the high $\delta^{15}N$ values of NH_4^+ at site P.

The soil NO_3^- $\delta^{15}N$ signals being mostly equal or higher than those of NH_4^+ in the CFPP region, and strictly lower in the OS region (mean isotopic difference between NH_4^+ and NO_3^- or $\Delta\delta^{15}N_{NH4+-NO3-}$, is −9‰), suggest that NO_3^- derived from nitrification of NH_4^+ does not dominate the bioavailable NO_3^- pools in the studied sites (Fig. 2A, B). Microbial nitrification is expected to generate NO_3^- $\delta^{15}N$ values lower than NH_4^+ (substrate) values under natural soil conditions (e.g., Pardo and Nadelhoffer, 2010). Instead, the NO_3^- values of the studied organic soil layers reflect a direct influence of the anthropogenic N inputs by surficial addition, with relatively high $\delta^{15}N$ values in the CFPP region and low values in the OS region (Fig. 2B).

The positive correlation between anthropogenic N inputs and pH found in the studied regions is intriguing. This correlation may be due

Table 3
Correlations (Spearman) between pH and alpha diversity indices.

Community	Soil layer	Shannon	Simpson	Richness
Soil bacteria	F	**0.58**	***0.41***	**0.70**
	H	**0.81**	**0.68**	**0.71**
	A	**0.87**	**0.77**	**0.75**
	B	**0.68**	**0.64**	**0.69**
Soil fungi	F	***0.42***	***0.41***	**0.55**
	H	0.17	0.08	0.00
	A	0.35	0.37	0.19
	B	0.21	0.17	0.26
Roo-tip EcM	F	n/a	n/a	0.09

Bold coefficients for 99.9% confidence level, bold italic, for 99%, and underlined, for 95%.

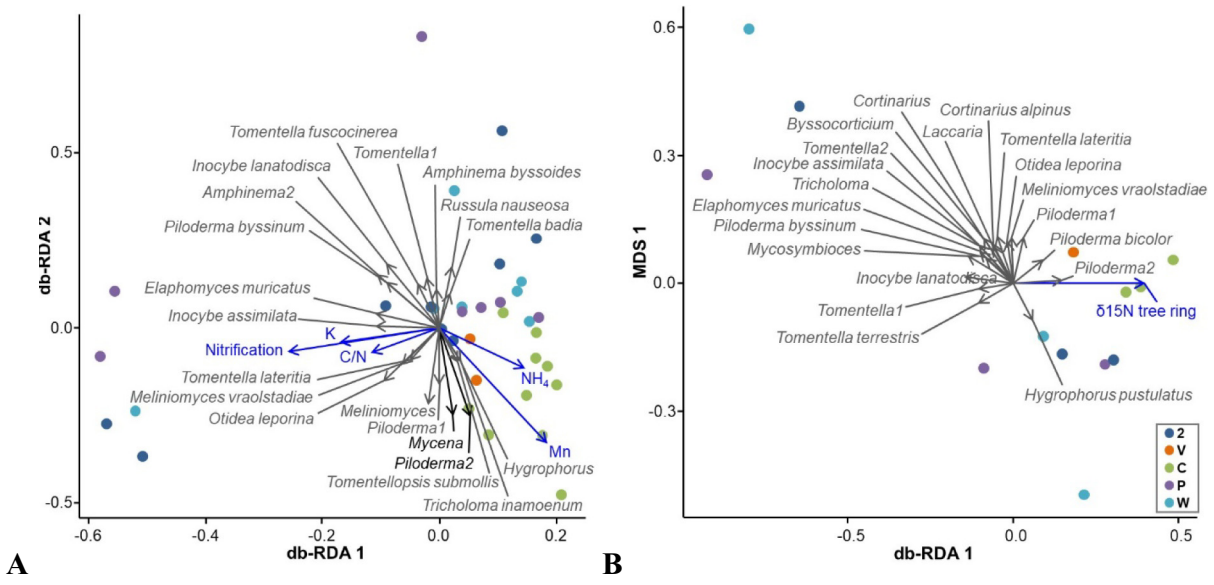

Fig. 7. Correlation triplots based on db-RDA using root-tip EcM community data constrained by the soil properties of the F horizon (A) and $\delta^{15}N$ in tree rings (B). Grey and black arrows represent an arrow length of 0.1 to 0.25, and 0.25 to 0.5, respectively (see legend of Fig. 5 for details).

to co-occurring trends, without reflecting a causal linkage. Or it may suggest that base cations accompanying the N emissions counteract the acidifying effects of depositing SOx and NOx or accentuate a pre-existing trends in pH values, with pH increasing with the deposition of alkaline fugitive dust (Wang et al., 2015; Mullan-Boudreau et al., 2017) at the most exposed site, as seen on lichens, soils, and peats of the OS region (Landis et al., 2012; Watmough et al., 2014; Fenn et al., 2015; Wieder et al., 2016). In the CFPP region, few nutrient data were available (NPRI, 2020), but indicated that the annual P and Mn emissions were 50% less and 25% more concentrated, respectively, than in the OS region. Moreover, differences in geological background have likely influenced the original soil pH. We cannot advocate a firmer interpretation with the current dataset. However, we can state that the anthropogenic emissions did not lower the pH in the studied sites.

4.2. The influence of soil biogeochemistry and pH

4.2.1. Different $\delta^{15}N$ values in EcM mantles

The general trend of increasing mantle $\delta^{15}N$ results with TDN $\delta^{15}N$ values reflects the overall assimilation of DON and NH_4^+ by EcM fungi, as NH_4^+ and DON mostly derive from TDN (Table 1, Section 3.1). As reported in the literature, EcM fungi markedly fractionate N due to preferential transfer of ^{14}N to roots (e.g., Gebauer and Taylor, 1999; Hobbie and Colpaert, 2002; Hobbie and Hogberg, 2012). This fractionation step generally enriches the EcM mantles in ^{15}N relative to their soil N sources. As NH_4^+ generally has much lower $\delta^{15}N$ values than TDN, the EcM mantle-assimilated N signals echo parent values between the NH_4^+ and TDN $\delta^{15}N$ values, making an almost 1:1 relationship between EcM fungi and TDN values (Fig. 4A).

At sites V and C, incorporation of NO_3^- that had $\delta^{15}N$ results lower than the ones of NH_4^+ (Fig. 2A, B) could have accounted for the mantle $\delta^{15}N$ values lower than the $\delta^{15}N$ values of NH_4^+, but at site P and near one tree at site W, NO_3^- had higher $\delta^{15}N$ values than NH_4^+, and cannot have accounted for the mantle $\delta^{15}N$ values lower than the NH_4^+ $\delta^{15}N$ values (Fig. 4A, B). It seems that there are local processes or other available N forms, perhaps specific low-$\delta^{15}N$ organic N compounds out of the bulk pool (Mayor et al., 2012), contributing to the N assimilated by EcM fungi at this site (Fig. 4C). Moreover, at high pH sites (2, P, W), the spread of EcM mantle $\delta^{15}N$ values relative to the TDN and NH_4^+ $\delta^{15}N$ trends, i.e., the broad $\Delta\delta^{15}N_{mantle\text{-}NH4+}$ range (Figs. 2A, 4A, B), and the variable NH_4^+ and EcM fungi relationship for the P and W sites (Fig. 4B) all suggest that EcM mantle exerted a different fractionation or assimilated NH_4^+ along with changing proportions of other soil N forms at these sites.

Specifically at the low-pH site C, TDN had much higher $\delta^{15}N$ values than NH_4^+ (Fig. A.3.2), mantle $\delta^{15}N$ values were high (+3.1‰), and $\delta^{15}N$ differences between mantle and NH_4^+ were the largest ($\Delta\delta^{15}N_{mantle\text{-}NH4+} = +3.9‰$). These observations suggest that EcM fungi did not dominantly assimilate NH_4^+, the favorite N compounds for spruce trees, but DON (Fig. 4A-C). Previous studies demonstrating that low pH favours EcM assimilation of DON support our interpretation (Abuzinadah and Read, 1986; Lilleskov et al., 2002; van der Linde et al., 2018). Moreover, the site C trees departing from all other trees in the graph of NH_4^+ and mantle $\delta^{15}N$ values (Fig. 4B) underline possible changes in the structure of the EcM communities at low pH (Fig. 3C, E; as suggested in Roth and Fahey, 1998, Kluber et al., 2012, Högberg et al., 2014).

4.2.2. Differences in microbial communities

The importance of the soil pH in driving the soil microbial communities observed in the current study is in line with numerous studies performed at continental (Fierer and Jackson, 2006) and local scales (Rousk et al., 2010), in different types of ecosystems (Fierer and Jackson, 2006), including forest soils (Lladó et al., 2018), although a stronger impact of pH on bacterial communities than on fungal communities is generally reported (Lauber et al., 2008). The high microbial diversity (Table A.6.1), relative abundance of bacterial taxa associated with nitrogen fixation, and nitrification rates in soils with high pH suggest that N-cycling processes could be diverse at sites P and W, supporting the interpretation based on soil and EcM $\delta^{15}N$ data (Fig. 4A–C; Section 4.2.1). Under such conditions, trees may assimilate N through direct root uptake or transfer from varied EcM genera such as *Piloderma* and *Meliniomyces*, with potentially large proportions from NH_4^+ in addition to DON.

The impact of pH on various N-cycling processes and associated microbial communities has been widely studied. In particular, a positive correlation between the soil pH, the abundance of nitrifying bacteria (Bru et al., 2011; Scarlett et al., 2020), and nitrification rates are commonly reported. The more complex relationship between mineralization and soil pH generally shows a U-shape, i.e., a decrease of

mineralization as pH increase up to ~6.0 followed by an increase of mineralization with pH increasing beyond 6 (e.g., Ste-Marie and Paré, 1999, and references therein). The pH of the F and H horizons studied here ranged between 3.6 and 6.8, likely explaining the inverse relation seen between pH and mineralization (Fig. 5A). Soil pH may also have a direct impact on N acquisition by trees, because at low soil pH, NH_4 uptake is limited as its absorption would lead to further acidification of soils through the release of H^+ (Rygiewicz et al., 1984). Under such acidic conditions, nitrate is not available, and DON components become important N sources for trees that can assimilate them directly (Näsholm et al., 2009) or through the contribution of EcM fungi having the capacity to use DON, such as *Piloderma* species (Heinonsalo et al., 2015).

The presence of three OTUs belonging to the genus *Piloderma*, developing hydrophobic mantles, in the F and H horizons of sites C, can partly explain the high EcM $\delta^{15}N$ values at these sites because $\delta^{15}N$ values associated with EcM fungi having hydrophobic hyphae are 3 to 4‰ higher than EcM fungi having hydrophilic hyphae values (Hobbie and Agerer, 2010), which is coherent with the $\Delta\delta^{15}N$ difference we observed for sites C and 2 in the OS region (Fig. 4C). Moreover, the presence in the F and H horizons of sites P and W of the EcM genus *Inocybe* developing hydrophilic mantles under high pH (Yang et al., 2018), supports the linkage between the types of EcM hyphae and tree-ring $\delta^{15}N$ values (Trudell et al., 2004). Of all studied sites, C and V received the lowest anthropogenic N inputs (Fig. A.4.1), which could favor the deployment of DON users (Mayor et al., 2012). Lilleskov et al. (2002) showed that *Piloderma* species tend to decline in frequency as atmospheric N inputs increased. Hydrophobic EcM fungi such as *Piloderma* tend to have proteolytic capabilities, and therefore the ability to decompose the main constituents of DON, amino acids or proteins (Hobbie and Hogberg, 2012; Chen et al., 2019; Lilleskov et al., 2019) that have high $\delta^{15}N$ values relative to NH_4^+. The multivariate analysis showed that *Piloderma* may have a key role in the EcM community at sites C and V. This analysis again supports the interpretation based on isotopic observations that EcM fungi dominantly assimilate DON at site C (Fig. 4A, B).

In contrast to soil fungi communities, the structure of EcM community colonizing the white spruce root tips did not directly change with soil pH (Table 3), but with the availability of some nutrients (Fig. 7A), which is linked to pH (Table 1). Previous studies have shown that fungi, including EcM fungi, tend to be tree-species specific and less influenced than bacteria by other soil physicochemical properties (Urbanova et al., 2015). Here, differences in tree species is ruled out because all EcM root tips analyzed were connected to white spruce trees and collected in their immediate vicinity, where soil samples were collected for pH determination. Nevertheless, as seen earlier, pH still seemed to have modulated the activities of EcM fungi because it correlated with $\delta^{15}N$ values of EcM mantles (Table 1; Fig. A.3.2.C).

Otherwise, the results obtained for EcM fungi from root tips support the general interpretation advocated for the results on soil fungi communities: (1) OTUs from the genus *Piloderma* also contributed significantly to the variation of the EcM community recovered from root tips in the most acidic sites C and V (pH < 5.5), and (2), at the less acidic sites, NH_4^+ was possibly immediately consumed along with other N forms by hydrophilic EcM fungi like *Inocybe*.

4.2.3. Tree-ring $\delta^{15}N$ values linked to soil pH

As seen in Sections 4.2.1 and 4.2.2, the EcM communities exerted different fractionations around the various trees or have different degrees of involvement during the N transfer from soils to roots. In both cases, the largest effects occurred at the most acidic sites, C and V, which in the end show much higher $\delta^{15}N$ values than sites 2, P and W. In regards to the next transfer step, the mantle and root $\delta^{15}N$ results support the interpretation in terms of various degrees of EcM fungi involvement during the assimilation of N by trees (Fig. 4C). The negligible fractionation during the N transfer from roots to tree rings (Fig. 4D) implies that tree-ring $\delta^{15}N$ results directly reflect the $\delta^{15}N$ values of N assimilated by roots. Hence, the assimilation by EcM fungi and root direct uptake of N compounds (mostly NH_4^+ and DON), with various $\delta^{15}N$ values will be transferred from roots to tree-ring $\delta^{15}N$ values. In other words, the ultimate tree-ring values will reflect variable proportions of the N forms taken up by the root-fungal association, and the various degrees of EcM fungi involvement during N assimilation. The N transfer by soil fungal communities, not analyzed for their $\delta^{15}N$ values, may also play in the N assimilation by roots at the studied sites.

The relationships of tree-ring $\delta^{15}N$ values with NH_4^+ concentration and pH (Table 2; Fig. 3C, D) indicated that N assimilated by trees integrates differences in availability and $\delta^{15}N$ signals of N compounds (Figs. 2A, 3A, B). Our results further suggest that the $\delta^{15}N$ signals in EcM mantles and tree rings were largely influenced by the N transformation rates (Table 1), themselves controlled by pH as suggested in Section 4.2.2 (Fig. A.4.1), and possibly anthropogenic inputs. These interpretation agree with previous findings on soil-N cycling stating that soil pH and N availability play key parts in regulating soil microbial communities and soil N dynamics (e.g., Ste-Marie and Paré, 1999; Lilleskov et al., 2002; Watmough, 2010; Kranabetter et al., 2013; Mayor et al., 2015; van der Linde et al., 2018; Etzold et al., 2020). In summary, the tree-ring $\delta^{15}N$-soil pH inverse correlation likely underlines the tree assimilation of N compounds with $\delta^{15}N$ values influenced by several biogeochemical processes.

4.3. Soil-to-tree N transfer processes inferred from the integrated datasets

We suggest that the anthropogenic N deposition partly contributes to generating distinct NO_3^- $\delta^{15}N$ clusters in the two studied regions, but do not control the soil NH_4^+ $\delta^{15}N$ signals or the ultimate tree-ring $\delta^{15}N$ values. At the regional scale, the positively correlating N deposition and soil pH may control differences in soil N dynamics, which are echoed in the present-day, large tree-ring $\delta^{15}N$ range. This interpretation uses the following arguments from the integrated datasets: (1) largely different $\delta^{15}N$ values in EcM mantle or tree rings occur in the same region (e.g., OS sites 2 and C), which all correlate inversely with pH, at the tree level, and with N deposition at the site level; (2) the soil-to-tree isotopic suite reveals that the NH_4^+ and DON (TDN) $\delta^{15}N$ values are transferred from soils to EcM fungi, roots, then to tree rings, sometimes bypassing EcM fungi; (3) high microbial diversity and nitrification rates play in determining soil N signals at the less acidic sites (2, P, W), which show low and broad $\delta^{15}N$ ranges in mantles and tree rings; (4) soil fungal OTUs of the genus *Piloderma* that are DON users, typically ^{15}N-rich relative to other soil fungi, are present at the most acidic sites (C and V) also receiving low amounts of anthropogenic N, where the mantle and tree-ring $\delta^{15}N$ values are the highest; (5) tree-ring $\delta^{15}N$ values correlate with the prevalence of *Piloderma* OTUs on white spruce root tips at these most acidic sites; and (6) the overall tree-ring $\delta^{15}N$ values correlate with pH at the site and tree scales.

These arguments derived from the soil N and EcM $\delta^{15}N$ relationships (Fig. 4A, B; Table 2), suggest that the EcM community structures and functions partially control the isotopic responses seen in white spruce trees at the various sites. This interpretation is further supported by the db-RDA of the overall soil fungal and EcM root-tip communities, which clearly identified several EcM OTUs associated with specific sites and significantly correlated with soil properties (pH, nutrient contents and N transformation rates).

The high diversity of bacteria in the high-pH sites (2, P and W) use up N copiously and nitrify, promoting a diversified N cycling with varied N pools bioavailable to EcM fungi and trees. Reduced reliance of trees on N transfer from EcM fungi at these sites under high pH and N deposition also plays an important role in producing the variable relationship between EcM mantle and root $\delta^{15}N$ values. Trees assimilate the several soil N forms either directly or through EcM fungi, except at low-pH sites where they dominantly assimilate DON through EcM fungi, producing the overall tree-ring $\delta^{15}N$ range observed. We summarize the dominating N-cycling patterns by low-$\delta^{15}N$ values for sites 2, P and W

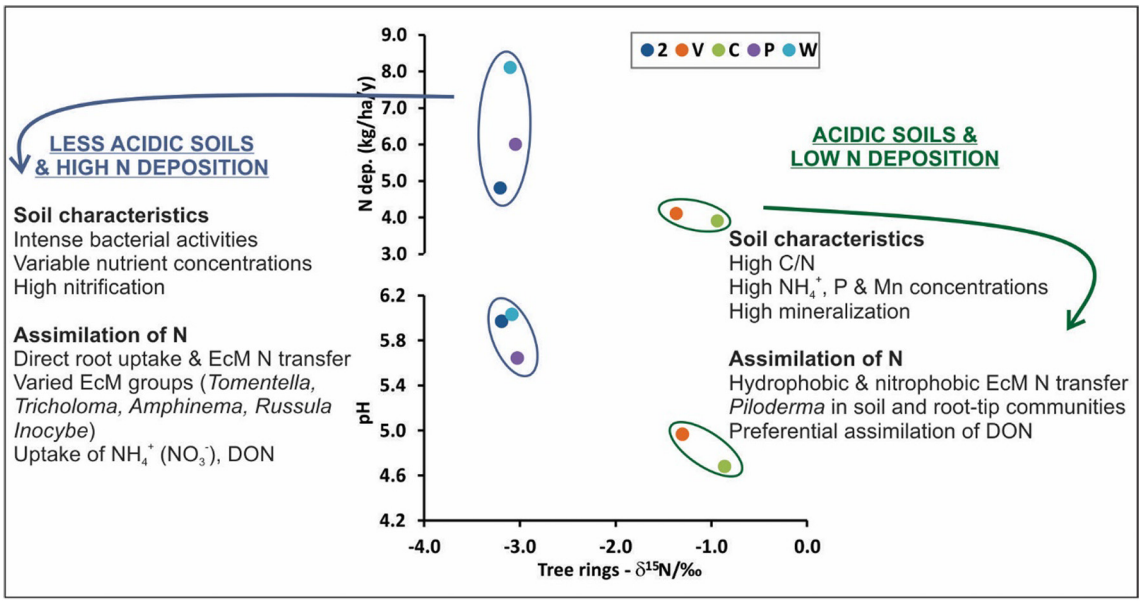

Fig. 8. Relationship of tree-ring $\delta^{15}N$ values with anthropogenic N deposition (dep.) (upper graph) and pH (lower graph) for the F and H horizons. The text summarizes the main N forms assimilated, assimilation modes and soil processes controlling the contrasted tree-ring $\delta^{15}N$ responses for sites 2, P, W (low $\delta^{15}N$) and V, C (high $\delta^{15}N$). Each tree-ring point per site represents the average for 15 measurements; each pH point, the average for 24 measurements (except site V, 8 measurements). The anthropogenic deposition is ground-verified modelled (Makar et al., 2018).

in responses to high pH and N deposition, and high-$\delta^{15}N$ values for sites C and V in response to low pH and N deposition (Fig. 8).

4.4. Implications of the described atmosphere-soil-tree N isotopic continuum

The soil results presented here indicate that the NO_3^- $\delta^{15}N$ values of surface soil partly reflect the distinct $\delta^{15}N$ signals of depositing airborne N in two separated regions, both exposed to moderate, chronic anthropogenic N inputs. The $\delta^{15}N$ values of other bioavailable N compounds, NH_4^+ and TDN (DON), do not reflect such effects. Given that white spruce trees favor the assimilation of soil NH_4^+, the studied tree rings did not record the distinct airborne anthropogenic $\delta^{15}N$ signals. Instead, as discussed in Section 4.3, they reflect soil conditions and processes dictated by pH and regional anthropogenic emissions (Fig. 8). In this sense our findings support the previous contention that tree-ring $\delta^{15}N$ values may express the characteristics of bioavailable N in soils (e.g., Högberg, 1997; Kranabetter et al., 2013; McLauchlan et al., 2017). In addition, co-pollutants such as base cations and SOx likely influenced as well the soil microbial dynamics and functions of trees (Siegwolf et al., 2021) through time (Savard et al., 2020a). However, determining these effects is beyond the scope of the present study.

The tree-ring $\delta^{15}N$ responses and the inferred causative processes presented here encourage revisiting the concept of signal transfer from pollutants to trees. This concept was invoked to interpret sets of data for several tree species exposed to emissions from large cities, vehicles, CFPP and industrial centers because they were generally from regions with high N deposition and their temporal trends converged towards the purported $\delta^{15}N$ values of anthropogenic emissions (Poulson et al., 1995, Saurer et al., 2004, Choi et al., 2005, Guerrieri et al., 2006, Bukata and Kyser, 2007, Kwak et al., 2009, Savard et al., 2009, Battipaglia et al., 2010, Doucet et al., 2011, Härdtle et al., 2013). However, other mechanisms than direct anthropogenic N assimilation by trees might play a role in modulating the tree-ring $\delta^{15}N$ trends. The results of the present study show that the EcM mantle $\delta^{15}N$ values directly reflect the soil N $\delta^{15}N$ values, but the spruce tree-ring $\delta^{15}N$ values do not. Instead, the overall tree-ring $\delta^{15}N$ values at the site scale suggest that biogeochemical soil conditions promote a partial switch from uptake through EcM fungi to direct root assimilation, as influenced by pH and anthropogenic N deposition (Fig. 8).

We showed here that the set of soil processes leading to the ultimate tree-ring $\delta^{15}N$ response to N inputs is complex. The industrial N inputs modified the surface soil NO_3^- $\delta^{15}N$ signals in the OS and CFPP regions, but this form of N was only rarely used in the high pH stands. The trees preferentially took up NH_4^+ from soils and this form of N largely varied in abundance and $\delta^{15}N$ values between sites. The overall NH_4^+ and TDN $\delta^{15}N$ values correlated with the ones recorded in EcM mantles, and the abundance of several EcM taxa significantly correlated with pH and N content. Moreover, our data suggest that trees largely obtained soil N through soil fungi and root-tip EcM transfers, but that they could have also assimilated N directly through their roots. Nonetheless, N deposition and soil pH appeared to embrace the numerous biogeochemical differences between sites driving the ultimate tree-ring $\delta^{15}N$ responses (Fig. 8). The integration of the data presented here allows us to conclude that ring $\delta^{15}N$ values of white spruce trees reflected multiple differences in environmental conditions.

4.5. Future lines of research

The Alberta study targeted a single species of trees with preference for NH_4^+ as soil N source, white spruce, to avoid species-specific effects on the EcM community structures, and root and tree-ring $\delta^{15}N$ values (McLauchlan and Craine, 2012; Pardo et al., 2013). In the future, the study of tree species with preference for NO_3^- assimilation (e.g., American beech, Templer and Dawson, 2004) may help assess if tree-ring $\delta^{15}N$ values of such tree species reflect the direct changes in soil NO_3^- $\delta^{15}N$ values imposed by anthropogenic N inputs. Continuing on the assimilation modes, quantifying the contribution of direct foliar N assimilation from ambient air relative to root uptake from soils to the total loads in stems and $\delta^{15}N$ values in tree rings would help refine our comprehension of tree-ring $\delta^{15}N$ ratios as environmental indicators. Studies should tackle this research question for various tree species. The study of a wider range of forest sites with highly contrasted soil pH values, such as black spruce stands usually growing on highly acidic soils, would help better discriminate the role of soil pH on N assimilation strategies by trees.

Future research using long tree-ring $\delta^{15}N$ series to provide a temporal perspective may help further assess the archival qualities of tree-ring $\delta^{15}N$ values for various anthropogenic N exposures and soil conditions. The results presented here linking the $\delta^{15}N$ values of recent tree rings with N deposition and soil pH along with the methodological approach for generating reliable long tree-ring series proposed in Savard et al. (2020b) suggest tree-ring $\delta^{15}N$ series should record middle- to long-term changes due to anthropogenic N inputs.

5. Conclusions

(1) Airborne anthropogenic moderate N inputs increased the amount of bioavailable N in soils and mostly modified the NO_3^- $\delta^{15}N$ values, but not those of NH_4^+, the preferred compounds of white spruce trees.
(2) The soil nutrient levels, N transformation rates, DIN and DON $\delta^{15}N$ values, bacteria and EcM community structures with various degrees of activities all interacted to produce a wide tree-ring $\delta^{15}N$ range, which in the end echoed differences in the main drivers for changes in soil conditions, which were pH and anthropogenic N deposition. In other words, soil conditions defined the microbial communities, which in turn governed the fractionation of soil N before its assimilation by trees.
(3) The recent tree-ring $\delta^{15}N$ values of boreal white spruce stands did not record direct airborne N signals, but they reflected site-specific biogeochemical responses and changes in soil N dynamics of the forests exposed to current anthropogenic N inputs.

The role of tree-ring series as archival system for anthropogenic perturbations of the forest N cycle can be further assessed by conducting research on long tree-ring series covering periods before and during industrial activities.

CRediT authorship contribution statement

Martine M. Savard: Funding acquisition, Conceptualization, Project administration, Supervision, Investigation, Resources, Formal analysis, Writing – original draft, Writing – review & editing, Visualization. **Christine Martineau:** Validation, Formal analysis, Writing – original draft, Writing – review & editing, Visualization. **Jérôme Laganière:** Funding acquisition, Conceptualization, Investigation, Resources, Writing – review & editing. **Christian Bégin:** Conceptualization, Investigation, Resources, Writing – review & editing. **Joëlle Marion:** Methodology, Investigation, Resources, Validation, Data curation. **Anna Smirnoff:** Methodology, Investigation, Validation, Data curation, Writing – review & editing. **Franck Stefani:** Conceptualization, Investigation, Writing – review & editing. **Jade Bergeron:** Methodology, Investigation, Writing – review & editing, Visualization. **Karelle Rheault:** Formal analysis, Data curation, Writing – review & editing, Visualization. **David Paré:** Conceptualization, Supervision, Writing – review & editing. **Armand Séguin:** Funding acquisition, Conceptualization, Supervision, Writing – review & editing.

Declaration of competing interest

The authors declare that they have no known competing financial interests or personal relationships that could have appeared to influence the work reported in this paper.

Acknowledgements

We thank Drs. A. Cole, P. Makar and R. Vet for constructive interaction on airborne N in Alberta. We acknowledge J. Beguin, S. Dagnault, M.-J. Morency, M. Luzincourt, P. Watt, F. Fournel, A. Bensadoune, J. Perreault, F. Michaud, O. Jeffrey and S. Rousseau for support during this research. We are grateful to Dr. J. Jautzy for a pre-submission review, and anonymous reviewers for constructive comments on the submitted manuscript. This research benefitted from the financial support by the Geological Survey of Canada Environmental Geoscience Program and the Canadian Forest Service Genomics R&D initiative and cumulative effects Program at NRCan, and from Environment & Climate Change Canada (Air Quality Division). This is NRCan contribution 20200628.

Appendix A. Supplementary data

Supplementary data to this article can be found online at https://doi.org/10.1016/j.scitotenv.2021.146581.

References

Abarenkov, K., Henrik Nilsson, R., Larsson, K.-H., Alexander, I.J., Eberhardt, U., et al., 2010. The UNITE database for molecular identification of fungi — recent updates and future perspectives. New Phytol. 186, 281–285.
Abuzinadah, R.A., Read, D.J., 1986. The role od proteins in the nitrogen nutrition of ectomycorrhizal plants I. Utilization of peptides and proteins by ectomycorrhizal fungi. New Phytol. 103, 481–493.
Averill, C., Finzi, A., 2011. Increasing plant use of organic nitrogen with elevation is reflected in nitrogen uptake rates and ecosystem $\delta^{15}N$. Ecology. 92, 883–891.
Battipaglia, G., Marzaioli, F., Lubritto, C., Altieri, S., Strumia, S., et al., 2010. Traffic pollution affects tree-ring width and isotopic composition of Pinus pinea. Sci. Total Environ. 408, 586–593.
Blanchet, F.G., Legendre, P., Borcard, D., 2008. Forward selection of explanatory variables. Ecology. 89, 2623–2632.
Bokulich, N.A., Subramanian, S., Faith, J.J., Gevers, D., Gordon, J.I., et al., 2013. Quality-filtering vastly improves diversity estimates from Illumina amplicon sequencing. Nat. Methods 10, 57–59.
Bru, D., Ramette, A., Saby, N.P.A., Dequiedt, S., Ranjard, L., et al., 2011. Determinants of the distribution of nitrogen-cycling microbial communities at the landscape scale. ISME J. 5, 532–542.
Bukata, A.R., Kyser, K.T., 2007. Carbon and nitrogen isotope variations in tree-rings as records of perturbations in regional carbon and nitrogen cycles. Environ. Sci. Technol. 41, 1331–1338.
Burnham, M.B., Adams, M.B., Peterjohn, W.T., 2019. Assessing tree ring $\delta^{15}N$ of four temperate deciduous species as an indicator of N availability using independent long-term records at the Fernow Experimental Forest, WV. Oecologia 191, 971–981.
Cabrera, M.L., Beare, M.H., 1993. Alkaline persulfate oxidation for determining total nitrogen in microbial biomass extracts. Soil Sci. Soc. Am. J. 57, 1007–1012.
Caporaso, J.G., Kuczynski, J., Stombaugh, J., Bittinger, K., Bushman, F.D., et al., 2010. QIIME allows analysis of high-throughput community sequencing data. Nat. Methods 7, 335–336.
Chase, J.M., Kraft, N.J.B., Smith, K.G., Vellend, M., Inouye, B.D., 2011. Using null models to disentangle variation in community dissimilarity from variation in α-diversity. Ecosphere 2 art24.
Chen, J., Heikkinen, J., Hobbie, E.A., Rinne-Garmston, K.T., Penttilä, R., et al., 2019. Strategies of carbon and nitrogen acquisition by saprotrophic and ectomycorrhizal fungi in Finnish boreal Picea abies-dominated forests. Fung. Biol. 123, 456–464.
Choi, W.-J., Lee, S.-M., Chang, S.X., Ro, H.-M., 2005. Variations of $\delta^{13}C$ and $\delta^{15}N$ in *Pinus Densiflora* tree-rings and their relationship to environmental changes in eastern Korea. Water Air Soil Pollut. 164, 173–187.
Courty, P.-E., Buée, M., Diedhiou, A.G., Frey-Klett, P., Le Tacon, F., et al., 2010. The role of ectomycorrhizal communities in forest ecosystem processes: new perspectives and emerging concepts. Soil Biol. Biochem. 42, 679–698.
Craine, J.M., Elmore, A.J., Aidar, M.P., Bustamante, M., Dawson, T.E., et al., 2009. Global patterns of foliar nitrogen isotopes and their relationships with climate, mycorrhizal fungi, foliar nutrient concentrations, and nitrogen availability. New Phytol. 183, 980–992.
Doucet, A., Savard, M.M., Bégin, C., Smirnoff, A., 2011. Is wood pre-treatment essential for tree-ring nitrogen concentration and isotope analysis? Rapid Commun. Mass Spectr. 25, 469–475.
Edgar, R.C., 2010. Search and clustering orders of magnitude faster than BLAST. Bioinformatics. 26, 2460–2461.
Edgar, R.C., 2013. UPARSE: highly accurate OTU sequences from microbial amplicon reads. Nat. Methods 10, 996–998.
Etzold, S., Ferretti, M., Reinds, G.J., Solberg, S., Gessler, A., et al., 2020. Nitrogen deposition is the most important environmental driver of growth of pure, even-aged and managed European forests. For. Ecol. Manag. 458, 117762.
Fenn, M.E., Bytnerowicz, A., Schilling, S.L., Ross, C.S., 2015. Atmospheric deposition of nitrogen, sulfur and base cations in jack pine stands in the Athabasca Oil Sands Region, Alberta, Canada. Environ. Pollut. 196, 497–510.
Fierer, N., Jackson, R.B., 2006. The diversity and biogeography of soil bacterial communities. Proc. Natl. Acad. Sci. U. S. A. 103, 626.
Gauthray-Guyénet, V., Schneider, R., Paré, D., Achim, A., Loi, C., et al., 2018. Influence of shifts over an 80-year period in forest composition on soil properties. Plant Soil 433, 111–125.
Gebauer, G., Taylor, A.F.S., 1999. ^{15}N natural abundance in fruit bodies of different functional groups of fungi in relation to substrate utilization. New Phytol. 142, 93–101.

Geng, L., Alexander, B., Cole-Dai, J., Steig, E.J., Savarino, J., et al., 2014. Nitrogen isotopes in ice core nitrate linked to anthropogenic atmospheric acidity change. Proc. Natl. Acad. Sci. U. S. A. 111, 5808–5812.
Gerhart, L.M., McLauchlan, K.K., 2014. Reconstructing terrestrial nutrient cycling using stable nitrogen isotopes in wood. Biogeochemistry. 120, 1–21.
Guerrieri, R., Vanguelova, E., Pitman, R., Benham, S., Perks, M., et al., 2020. Climate and atmospheric deposition effects on forest water-use efficiency and nitrogen availability across Britain. Sci Rep. 10, 12418.
Härdtle, W., Niemeyer, T., Assmann, T., Baiboks, S., Fichtner, A., et al., 2013. Long-term trends in tree-ring width and isotope signatures ($\delta^{13}C$, $\delta^{15}N$) of Fagus sylvatica L. on soils with contrasting water supply. Ecosystems. 16, 1413–1428.
Heinonsalo, J., Sun, H., Santalahti, M., Bäcklund, K., Hari, P., et al., 2015. Evidences on the ability of mycorrhizal genus *Piloderma* to use organic nitrogen and deliver it to Scots pine. PLoS One 10, e0131561.
Hemsley, T.L., MacKenzie, M.D., Quideau, S.A., 2019. Ecophysiological response of aspen (*Populus tremuloides*) and jack pine (*Pinus banksiana*) to atmospheric nitrogen deposition on reconstructed boreal forest soils in the Athabasca oil sands region. Sci. Total Environ. 696, 133544.
Herlemann, D.P.R., Labrenz, M., Jürgens, K., Bertilsson, S., Waniek, J.J., et al., 2011. Transitions in bacterial communities along the 2000 km salinity gradient of the Baltic Sea. ISME J. 5, 1571–1579.
Hobbie, E., Colpaert, J., 2002. Nitrogen availability and colonization by mycorrhizal fungi correlate with nitrogen isotope patterns in plants. New Phytol. 157.
Hobbie, E.A., Agerer, R., 2010. Nitrogen isotopes in ectomycorrhizal sporocarps correspond to belowground exploration types. Plant Soil 327, 71–83.
Hobbie, E.A., Hogberg, P., 2012. Nitrogen isotopes link mycorrhizal fungi and plants to nitrogen dynamics. New Phytol. 196, 367–382.
Hobbie, E.A., Ouimette, A.P., 2009. Controls of nitrogen isotope patterns in soil profiles. Biogeochemistry. 95, 355–371.
Hobbie, E.A., Jumpponen, A., Trappe, J., 2005. Foliar and fungal ^{15}N:^{14}N ratios reflect development of mycorrhizae and nitrogen supply during primary succession: testing analytical models. Oecologia. 146, 258–268.
Högberg, P., 1997. Tansley review no. 95. ^{15}N natural abundance in soil-plant systems. New Phytol. 137, 179–203.
Högberg, P., Johannisson, C., Yarwood, S., Callesen, I., Nasholm, T., et al., 2011. Recovery of ectomycorrhiza after 'nitrogen saturation' of a conifer forest. New Phytol. 189, 515–525.
Högberg, P., Johannisson, C., Högberg, M., 2014. Is the high ^{15}N natural abundance of trees in N-loaded forests caused by an internal ecosystem N isotope redistribution or a change in the ecosystem N isotope mass balance? Biogeochemistry. 117.
Islam, M.A., Macdonald, S.E., 2009. Current uptake of ^{15}N-labeled ammonium and nitrate in flooded and non-flooded black spruce and tamarack seedlings. Ann. For. Sci. 66, 1–11.
Kluber, L.A., Carrino-Kyker, S.R., Coyle, K.P., DeForest, J.L., Hewins, C.R., et al., 2012. Mycorrhizal response to experimental pH and P manipulation in acidic hardwood forests. PLoS One 7, e48946.
Kranabetter, J.M., Saunders, S., MacKinnon, J.A., Klassen, H., Spittlehouse, D.L., 2013. An assessment of contemporary and historic nitrogen availability in contrasting coastal Douglas-fir forests through $\delta^{15}N$ of tree rings. Ecosystems. 16, 111–122.
Kuang, Y., Sun, F., Wen, D., Xu, Z., Huang, L., et al., 2011. Nitrogen deposition influences nitrogen isotope composition in soil and needles of Pinus massoniana forests along an urban-rural gradient in the Pearl River Delta of south China. J. Soils Sediments 11, 589–595.
Kwak, J.-H., Choi, W.-J., Lim, S.-S., Arshad, M.A., 2009. $\delta^{13}C$, $\delta^{15}N$, N concentration, and ca-to-Al ratios of forest samples from Pinus densiflora stands in rural and industrial areas. Chem. Geol. 264, 385–393.
Lauber, C.L., Strickland, M.S., Bradford, M.A., Fierer, N., 2008. The influence of soil properties on the structure of bacterial and fungal communities across land-use types. Soil Biol. Biochem. 40, 2407–2415.
Lilleskov, E.A., Fahey, T.J., Horton, T.R., Lovett, G.M., 2002. Belowground ectomycorrhizal fungal community change over a nitrogen deposition gradient in Alaska. Ecology. 83, 104–115.
Lilleskov, E.A., Kuyper, T.W., Bidartondo, M.I., Hobbie, E.A., 2019. Atmospheric nitrogen deposition impacts on the structure and function of forest mycorrhizal communities: a review. Environ. Pollut. 246, 148–162.
van der Linde, S., Suz, L.M., Orme, C.D.L., Cox, F., Andreae, H., et al., 2018. Environment and host as large-scale controls of ectomycorrhizal fungi. Nature. 558, 243–248.
Liu, X.-Y., Koba, K., Makabe, A., Li, X.-D., Yoh, M., et al., 2013. Ammonium first: natural mosses prefer atmospheric ammonium but vary utilization of dissolved organic nitrogen depending on habitat and nitrogen deposition. New Phytol. 199, 407–419.
Lladó, S., López-Mondéjar, R., Baldrian, P., 2018. Drivers of microbial community structure in forest soils. Appl. Microbiol. Biotechnol. 102, 4331–4338.
Makar, P.A., Akingunola, A., Aherne, J., Cole, A.S., Aklilu, Y.-A., et al., 2018. Estimates of exceedances of critical loads for acidifying deposition in Alberta and Saskatchewan. Atmos. Chem. Phys. 18, 9897–9927.
Mathias, J.M., Thomas, R.B., 2018. Disentangling the effects of acidic air pollution, atmospheric CO_2 , and climate change on recent growth of red spruce trees in the Central Appalachian Mountains. Global Change Biol. 3938–3953.
Mayor, J.R., Schuur, E.A.G., Mack, M.C., Hollingsworth, T.N., Bååth, E., 2012. Nitrogen isotope patterns in Alaskan black spruce reflect organic nitrogen sources and the activity of ectomycorrhizal Fungi. Ecosystems. 15, 819–831.
Mayor, J.R., Wright, S.J., Schuur, E.A.G., Brooks, M.E., Turner, B.L., 2014. Stable nitrogen isotope patterns of trees and soils altered by long-term nitrogen and phosphorus addition to a lowland tropical rainforest. Biogeochemistry. 119, 293–306.
Mayor, J.R., Mack, M.C., Schuur, E.A.G., 2015. Decoupled stoichiometric, isotopic, and fungal responses of an ectomycorrhizal black spruce forest to nitrogen and phosphorus additions. Soil Biol. Biochem. 88, 247–256.
McDonald, D., Price, M.N., Goodrich, J., Nawrocki, E.P., DeSantis, T.Z., et al., 2012. An improved Greengenes taxonomy with explicit ranks for ecological and evolutionary analyses of bacteria and archaea. ISME J. 6, 610–618.
McLauchlan, K.K., Craine, J.M., 2012. Species-specific trajectories of nitrogen isotopes in Indiana hardwood forests, USA. Biogeosciences. 9, 867–874.
McLauchlan, K.K., Craine, J.M., Oswald, W.W., Leavitt, P.R., Likens, G.E., 2007. Changes in nitrogen cycling during the past century in a northern hardwood forest. Proc. Natl. Acad. Sci. 104, 7466.
McLauchlan, K.K., Gerhart, L.M., Battles, J.J., Craine, J.M., Elmore, A.J., et al., 2017. Centennial-scale reductions in nitrogen availability in temperate forests of the United States. Sci. Rep. 7.
Mullan-Boudreau, G., Belland, R., Devito, K., Noernberg, T., Pelletier, R., et al., 2017. Sphagnum moss as an indicator of contemporary rates of atmospheric dust deposition in the Athabasca bituminous sands region. Environ. Sci. Technol. 51, 7422–7431.
Näsholm, T., Kielland, K., Ganeteg, U., 2009. Uptake of organic nitrogen by plants. New Phytol. 182, 31–48.
Nguyen, N.H., Song, Z., Bates, S.T., Branco, S., Tedersoo, L., et al., 2016. FUNGuild: an open annotation tool for parsing fungal community datasets by ecological guild. Fungal Ecol. 20, 241–248.
Pardo, L.H., Semaoune, P., Schaberg, P.G., Eagar, C., Sebilo, M., 2013. Patterns in $\delta^{15}N$ in roots, stems, and leaves of sugar maple and American beech seedlings, saplings, and mature trees. Biogeochemistry. 112, 275–291.
Poulson, S.R., Chamberlain, C.P., Friedland, A.J., 1995. Nitrogen isotope variation of tree rings as a potential indicator of environmental change. Chem. Geol. 125, 307–315.
Proemse, B.C., Mayer, B., Fenn, M.E., Ross, C.S., 2013. A multi-isotope approach for estimating industrial contributions to atmospheric nitrogen deposition in the Athabasca oil sands region in Alberta, Canada. Environ. Pollut. 182, 80–91.
Roth, D.R., Fahey, T.J., 1998. The effects of acid precipitation and ozone on the Ectomycorrhizae of red spruce saplings. Water Air Soil Pollut. 103, 263–276.
Rousk, J., Bååth, E., Brookes, P.C., Lauber, C.L., Lozupone, C., et al., 2010. Soil bacterial and fungal communities across a pH gradient in an arable soil. ISME J. 4, 1340–1351.
Rygiewicz, P.T., Bledsoe, C.S., Zasoski, R.J., 1984. Effects of ectomycorrhizae and solution pH on [^{15}N]ammonium uptake by coniferous seedlings. Can. J. For. Res. 14, 885–892.
Saurer, M., Cherubini, P., Ammann, M., De Cinti, B., Siegwolf, R., 2004. First detection of nitrogen from NOx in tree rings: a $^{15}N/^{14}N$ study near a motorway. Atmos. Environ. 38, 2779–2787.
Savard, M.M., Bégin, C., Smirnoff, A., Marion, J., Rioux-Paquette, E., 2009. Tree-ring nitrogen isotopes reflect anthropogenic NOX emissions and climatic effects. Environ. Sci. Technol. 43, 604–609.
Savard, M.M., Cole, A., Smirnoff, A., Vet, R., 2017. $\delta^{15}N$ values of atmospheric N species simultaneously collected using sector-based samplers distant from sources — isotopic inheritance and fractionation. Atmos. Environ. 162, 11–22.
Savard, M.M., Bégin, C., Marion, J., 2020a. Response strategies of boreal spruce trees to anthropogenic changes in air quality and rising pCO_2. Environ. Pollut. 261, 114209.
Savard, M.M., Marion, J., Bégin, C., 2020b. Nitrogen isotopes of individual tree-ring series — the validity of middle- to long-term trends. Dendrochronologia. 62, 125726.
Scarlett, K., Denman, S., Clark, D.R., Forster, J., Vanguelova, E., et al., 2020. Relationships between nitrogen cycling microbial community abundance and composition reveal the indirect effect of soil pH on oak decline. ISME J. 15, 623–635.
Schleppi, P., Bucher-Wallin, I., Saurer, M., Jäggi, M., Landolt, W., 2006. Citric acid traps to replace sulphuric acid in the ammonia diffusion of dilute water samples for ^{15}N analysis. Rapid Commun. Mass Spectrom. 20, 629–634.
Schloss, P.D., Westcott, S.L., Ryabin, T., Hall, J.R., Hartmann, M., et al., 2009. Introducing mothur: open-source, platform-independent, community-supported software for describing and comparing microbial communities. Appl. Environ. Microbiol. 75, 7537.
Sebilo, M., Mayer, B., Grably, M., Billiou, D., Mariotti, A., 2004. The use of the ammonium diffusion method for $\delta^{15}N$-NH_4^+ and $\delta^{15}N$-NO_3^- measurements: comparison with other techniques. Environ. Chem. 1, 99–103.
Smirnoff, A., Savard, M.M., Vet, R., Simard, M.C., 2012. Nitrogen and triple oxygen isotopes in near-road air samples using chemical conversion and thermal decomposition. Rapid Commun. Mass Spectrom. 26, 2791–2804.
Stefani, F., Isabel, N., Morency, M.-J., Lamothe, M., Nadeau, S., et al., 2018. The impact of reconstructed soils following oil sands exploitation on aspen and its associated belowground microbiome. Sci. Rep. 8, 2761.
Ste-Marie, C., Paré, D., 1999. Soil, pH and N availability effects on net nitrification in the forest floors of a range of boreal forest stands. Soil Biol. Biochem. 31, 1579–1589.
Succarie, A., Xu, Z., Wang, W., Liu, T., Zhang, X., et al., 2020. Effects of climate change on tree water use efficiency, nitrogen availability and growth in boreal forest of northern China. J. Soils Sediments 20, 3607–3614.
Templer, P., Dawson, T.E., 2004. Nitrogen uptake by four tree species of the Catskill Mountains, New York: implications for forest N dynamics. Plant Soil 262, 251–261.
Thiffault, E., Paré, D., Bélanger, N., Munson, A., Marquis, F., 2006. Harvesting intensity at clear-felling in the boreal forest. Soil Sci. Soc. Am. J. 70, 691–701.
Toju, H., Tanabe, A.S., Yamamoto, S., Sato, H., 2012. High-coverage ITS primers for the DNA-based identification of Ascomycetes and Basidiomycetes in environmental samples. PLoS One 7, e40863.
Tomlinson, G., Buchmann, N., Siegwolf, R., Weber, P., Thimonier, A., et al., 2015. Can tree-ring $\delta^{15}N$ be used as a proxy for foliar $\delta^{15}N$ in European beech and Norway spruce? Trees. 30, 627–638.
Trudell, S.A., Rygiewicz, P.T., Edmonds, R.L., 2004. Patterns of nitrogen and carbon stable isotope ratios in macrofungi, plants and soils in two old-growth conifer forests. New Phytol. 164, 317–335.

Wang, X., Chow, J.C., Kohl, S.D., Percy, K.E., Legge, A.H., et al., 2015. Characterization of $PM_{2.5}$ and PM_{10} fugitive dust source profiles in the Athabasca Oil Sands Region. J. Air Waste Manag. Assoc. 65, 1421–1433.

Watmough, S.A., 2010. An assessment of the relationship between potential chemical indices of nitrogen saturation and nitrogen deposition in hardwood forests in southern Ontario. Environ. Monit. Assess. 164, 9–20.

Watmough, S.A., Whitfield, C.J., Fenn, M.E., 2014. The importance of atmospheric base cation deposition for preventing soil acidification in the Athabasca Oil Sands Region of Canada. Sci. Total Environ. 493, 1–11.

Wieder, R.K., Vile, M.A., Albright, C.M., Scott, K.D., Vitt, D.H., et al., 2016. Effects of altered atmospheric nutrient deposition from Alberta oil sands development on Sphagnum fuscum growth and C, N and S accumulation in peat. Biogeochemistry. 129, 1–19.

Xu, Y., Xiao, H., Wu, D., 2019. Traffic-related dustfall and NOx, but not NH3, seriously affect nitrogen isotopic compositions in soil and plant tissues near the roadside. Environ. Pollut. 249, 655–665.

Yang, N., Butenschoen, O., Rana, R., Koehler, L., Hertel, D., et al., 2018. Leaf litter species identity influences biochemical composition of ectomycorrhizal fungi. Mycorrhiza. 29, 85–96.

Uncategorized references

Canadian Society of Soil Science, 2020. Soils of Canada. [Online]. https://soilsofcanada.ca/citation.php.

Carter, M.R., Gregorich, E.G., 2007. Soil Sampling and Methods of Analysis. 2nd ed. CRC Press, Boca Raton https://doi.org/10.1201/9781420005271.

Guerrieri, R.M., Saurer, M., Siegwolf, R., Waldner, P., Cherubini, P., 2006. Impatto del traffico veicolare su $\delta^{15}N$, $\delta^{13}C$ e $\delta^{18}O$ di aghi ed anelli annuali di abete rosso (*Picea abies* L.) presso un'autostrada in Svizzera. Ed..

Hair, J.F., 2011. Multivariate data analysis: an overview. Chap. In: Lovric, M. (Ed.), International Encyclopedia of Statistical Science. Springer Berlin Heidelberg, Berlin, Heidelberg, pp. 904–907.

Handley, L.L., Scrimgeour, C.M., Raven, J.A., 1998. ^{15}N natural abundance levels in terrestrial vascular plants: a précis. In: Griffiths, H. (Ed.), Stable Isotopes: Integration of Biological, Ecological and Geochemical Processes. Bios Scientific Publishers, Oxford, UK.

Hannon, J.E., Böhlke, J.K., 2008. Determination of the $\delta(^{15}N/^{14}N)$ of ammonium (NH_4^+) in water: RSIL lab code 2898, chap. C15. In: Révész, K., Coplen, Tyler B. (Eds.), Methods of the Reston Stable Isotope Laboratory: U.S. Geological Survey, Techniques and Methods. United States Geological Survey, pp. 1–30.

Illumina, 2013. 16S metagenomic sequencing library preparation. [Online]. https://support.illumina.com/content/dam/illumina-support/documents/documentation/chemistry_documentation/16s/16s-metagenomic-library-prep-guide-15044223-b.pdf.

Landis, M.S., Pancras, J.P., Graney, J.R., Stevens, R.K., Percy, K.E., et al., 2012. Chapter 18 — Receptor modeling of epiphytic lichens to elucidate the sources and spatial distribution of inorganic air pollution in the Athabasca Oil Sands Region. In: Percy, K.E. (Ed.), Alberta Oil Sands — Energy, Industry and the Environment. Developments in Environmental Science. Elsevier, pp. 427–467.

Nadelhoffer, K., Fry, B., 1988. Controls on Natural Nitrogen-15 and Carbon-13 Abundances in Forest Soil Organic Matter. Ed. https://doi.org/10.2136/sssaj1988.03615995005200060024x.

NPRI, 2020. National pollutant release inventory. [Online]. https://www.canada.ca/en/services/environment/pollution-waste-management/national-pollutant-release-inventory.html.

Oksanen, J., Kindt, R., Legendre, P., O'Hara, B., Stevens, M.H.H., 2007. The vegan package. [Online]. http://cran.r-project.org/ http://r-forge.r-project.org/projects/vegan/.

Pardo, L.H., Nadelhoffer, K.J., 2010. Using nitrogen isotope ratios to assess terrestrial ecosystems at regional and global scales. In: West, J.B., Bowen, G.J., Dawson, T.E., Tu, K.P. (Eds.), Isoscapes: Understanding Movement, Pattern, and Process on Earth Through Isotope Mapping. Springer Netherlands, Dordrecht, pp. 221–249.

R-Core-Team, 2019. A Language and Environment for Statistical Computing. R Foundation for Statistical Computing [Online]. https://www.R-project.org.

Revelle, W.R., 2020. psych: procedures for personality and psychological research. [Online]. https://CRAN.R-project.org/package=psych.

Savard, M.M., Siegwolf, R.T.W., 2021. Chapter 12 — nitrogen isotopes in tree rings – challenges and prospect. In: RTW, Siegwolf, Brooks, J., Roden, J., Saurer, M. (Eds.), Stable Isotopes in Tree Rings: Inferring Physiological, Climatic and Environmental Responses. Springer.

Siegwolf, R.T.W., Savard, M.M., Grams, T.E.E., Voelker, S., 2021. Impact of increasing CO_2, and air pollutants (NOx, SO_2, O_3) on the stable isotope ratios in tree rings. In: Siegwolf, R.T.W., Brooks, J., Roden, J., Saurer, M. (Eds.), Stable Isotopes in Tree Rings: Inferring Physiological, Climatic and Environmental Responses. Springer.

Wickhame, H., 2016. In: Publishing, S.I. (Ed.), ggplot2: Elegant Graphics for Data Analysis Use R!, 2nd ed. Springer-Verlag, New York.